

Crystallography and Crystalline Defects

6.1 Introduction

Integrated circuits are fabricated on single-crystal wafers sliced from semiconductor ingots. The chemical properties (such as etch rates) and physical properties (such as cleavage planes) of the semiconductors depend on its crystallographic directions and planes. Wafers are commonly identified by their surface orientation and reference flats cut on the edges. Figure 6.1 shows a Si wafer with a reference flat. The flat of this material is used to denote the $\langle 110 \rangle$ direction or the cleavage planes. If scribe lines are drawn on wafers parallel to the reference flats with a pointed tool, the wafer may be cleaved easily along the scribe lines.

To improve the quality of the material on which the devices are built, an epitaxial growth process is often used. This process is a technique to grow a thin crystalline layer on a crystalline substrate (Fig. 6.2) so that the grown layer bears a certain crystallographic relationship with respect to the underlying substrate. Epitaxy not only offers the possibility of reducing defect density and unwanted impurities in the crystalline layers, but also has the advantage of providing layers of different doping concentrations and carrier types than those in the substrate. In Si technology, the epitaxial layer is Si; this type of epitaxy is termed homoepitaxy. In GaAs and other III-V compound technology, heteroepitaxy is often practiced, such as growing $Al_xGa_{1-x}As$ epitaxial layers on GaAs, as discussed in Chapters 13 and 14. The emphasis in this chapter is on the crystal lattice and the defects present in semiconductors. These defects play a major role in semiconductor technology.

6.2 Crystallography

Semiconductor wafers, even without any epitaxial layers, contain imperfections. Defects in a crystalline material can be categorized as (1) point defects, (2) line defects, (3) planar defects, and (4) volume defects. These defects will be characterized in the following sections. Although defects are generally undesirable and often unavoidable in a crystal, in some cases they can be put to use to improve the device performance, such as in defect “gettering” of unwanted impurities. To characterize crystalline defects, a certain amount of crystallography is necessary.

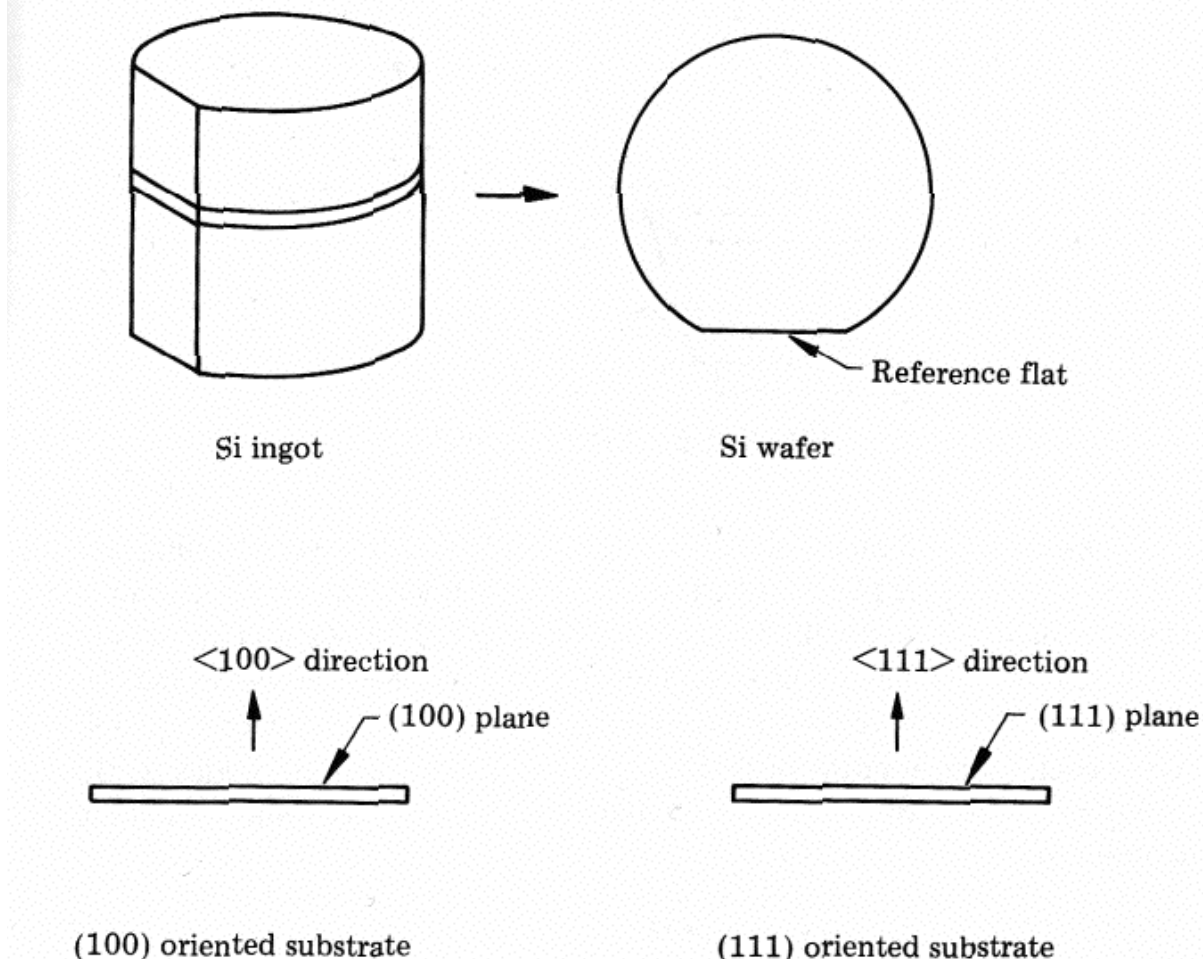


FIGURE 6.1 Schematics showing a Si wafer cut from a Si ingot. The reference flat denotes the $\langle 110 \rangle$ direction. For (100)-oriented substrates, the $\langle 110 \rangle$ direction is the line of intersection between a (111) plane and the surface (100) plane. There are two orthogonal sets of $\langle 110 \rangle$ directions on a (100) plane. For (111)-oriented substrates, the $\langle 110 \rangle$ direction is the line of intersection between another (111) plane and the surface (111) plane. There are three sets of $\langle 110 \rangle$ directions on a (111) surface making 60° angles with each other.

A crystal is a solid composed of atoms arranged in a pattern periodic in space. It is, however, sometimes more convenient to consider a set of points to define crystals. Such a set of points, called lattice points, have a fixed relation in space, meaning that the lattice when viewed in a particular direction from one lattice point would appear exactly the same when viewed in the same direction from *any other* lattice point. This set of points is defined such that each point in this array has identical surroundings. The lattice points usually coincide with atom positions. However, in complicated crystals, the individual atoms may not have identical surroundings, whereas the lattices describing the complicated crystals will. Because

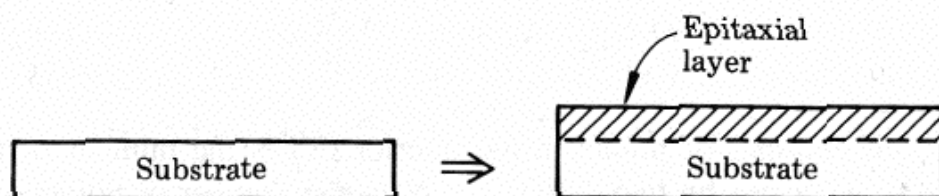
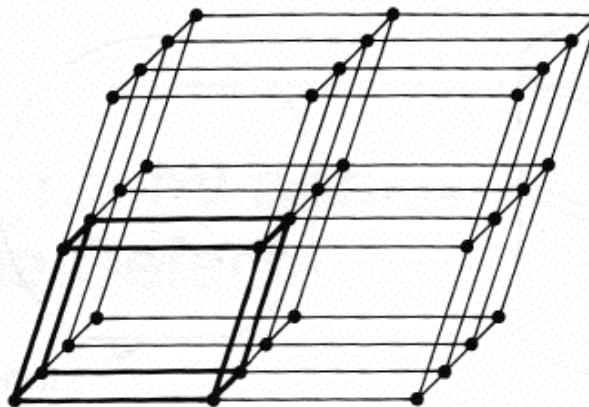


FIGURE 6.2 Growth of epitaxial layers.

**FIGURE 6.3** Point lattice.

of this property of a lattice point, the space containing this set of points can be divided by three sets of planes into a set of cells each identical in size, shape, and orientation; such a cell is called a unit cell. Figure 6.3 shows a point lattice; the heavy dark lines outline a unit cell. This cell repeats itself in space and can be described by three unit vectors \mathbf{a} , \mathbf{b} , and \mathbf{c} , called crystallographic axes, that are related to each other in terms of their lengths a , b , and c and the angles α , β , and γ (see Fig. 6.4). Any direction in the cell can be described as a linear combination of the three axes:

$$\mathbf{r} = n_1\mathbf{a} + n_2\mathbf{b} + n_3\mathbf{c}. \quad (6.1)$$

In addition,

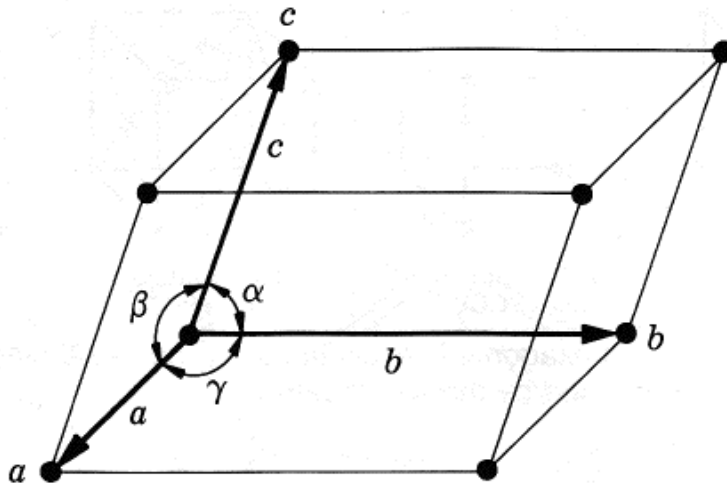
$$\mathbf{r} = \mathbf{r}_0 + P\mathbf{a} + Q\mathbf{b} + R\mathbf{c} \quad (6.2)$$

where P , Q , and R are integers. This means that the unit cell may be translated in space via a linear combination of the unit vectors without changing the surroundings (i.e., the unit cell repeats itself in space).

In dividing the space by three sets of planes, various shapes and sizes of unit cells can be produced. As it turns out, only seven different kinds of cells are necessary to describe all possible point lattices. These seven kinds of cells define seven crystal systems, shown in Fig. 6.4. Each corner of the unit cell of these seven systems has a lattice point, but not in the interior of the cells or on the cell faces. It is possible to place more points either in the center of the unit cell or on the cell faces without violating the general definition of a point lattice that each has identical surroundings for certain crystal systems. Based on this arrangement of points, a total of 14 so-called Bravais lattices can be produced for the seven crystal systems. Figure 6.5 shows four of these lattices: the cubic and hexagonal Bravais lattices. The number of lattice points in a unit cell, N_u , is given by

$$N_u = N_i + \frac{N_f}{2} + \frac{N_c}{8} \quad (6.3)$$

where N_i is the number of points in the interior, N_f is the number of points on faces (each N_f is shared by two cells), and N_c is the number of points on corners (each N_c point is shared by eight cells). When $N_u = 1$, the cell is called a primitive



System	Axial lengths and angles	Bravais lattice
Cubic	Three equal axes at right angles $a = b = c, \alpha = \beta = \gamma = 90^\circ$	Simple Body-centered Face-centered
Tetragonal	Three axes at right angles, two equal $a = b \neq c, \alpha = \beta = \gamma = 90^\circ$	Simple Body-centered
Orthorhombic	Three unequal axes at right angles $a \neq b \neq c, \alpha = \beta = \gamma = 90^\circ$	Simple Body-centered Base-centered Face-centered
Rhombohedral*	Three equal axes, equally inclined $a = b = c, \alpha = \beta = \gamma \neq 90^\circ$	Simple
Hexagonal	Two equal coplanar axes at 120° , third axis at right angles $a = b \neq c, \alpha = \beta = 90^\circ, \gamma = 120^\circ$	Simple
Monoclinic	Three unequal axes, one pair not at right angles $a \neq b \neq c, \alpha = \gamma = 90^\circ \neq \beta$	Simple Base-centered
Triclinic	Three unequal axes, unequally inclined and none at right angles $a \neq b \neq c, \alpha \neq \beta \neq \gamma \neq 90^\circ$	Simple

*Also called trigonal.

FIGURE 6.4 Unit cell and the seven crystal systems.

cell. A unit cell is not necessarily a primitive cell; however, any nonprimitive unit cell can be “referred” to a primitive cell, as shown in Fig. 6.6.

In considering the Bravais lattice of the face-centered cubic lattice shown in Fig. 6.6, it is customary to use the conventional unit cell of the FCC cell rather than the primitive cell. Since it is a cubic system ($a = b = c, \alpha = \beta = \gamma = 90^\circ$) the length a is called the lattice parameter. The number of atoms per unit cell with $N_i = 0, N_f = 6$, and $N_c = 8$ is

$$N_u = \frac{6}{2} + \frac{8}{8} = 4 \text{ atoms/unit cell.} \quad (6.4a)$$

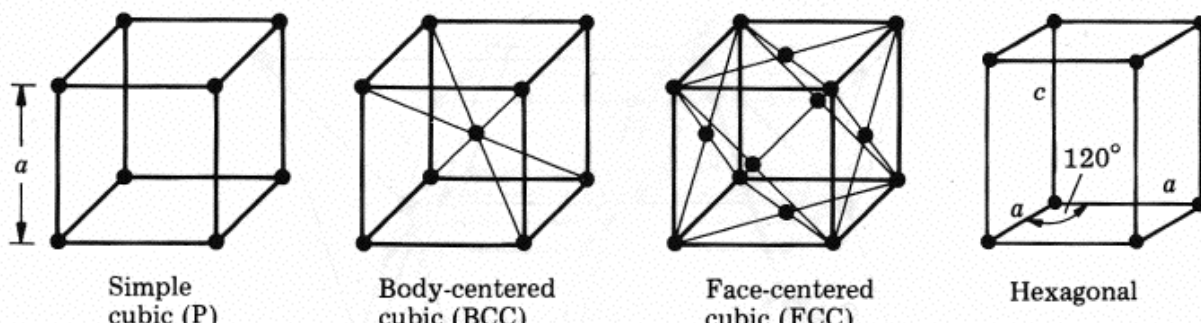


FIGURE 6.5 Cubic and hexagonal Bravais lattices. The basal plane of a hexagonal lattice is the plane defined by the two a axes.

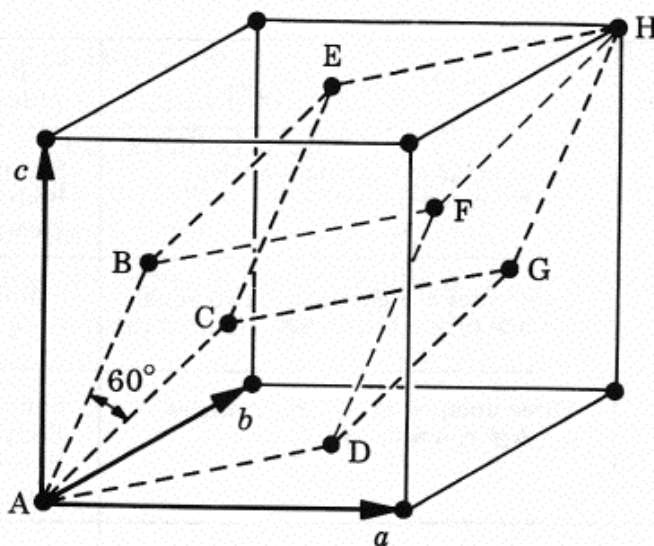


FIGURE 6.6 Face-centered cubic point lattice referred to a rhombohedral primitive cell. The FCC unit cell is shown by the solid lines. The rhombohedral primitive cell is outlined by the dashed lines. Points A and H are on the corners of the FCC cell as well as of the rhombohedral cell; points B, C, D, E, F, and G are on the corners of the rhombohedral cell but on the faces of the FCC cell. [After Cullity (1956).]

A number of commonly used metals in IC technology belong to the FCC crystal structure, such as Al ($a = 0.405$ nm) and Au ($a = 0.408$ nm). Many semiconductors have a diamond cubic structure, which is not one of the Bravais lattices. The diamond structure can be considered to be two interpenetrating FCC lattices with two atoms associated with one lattice point. The diamond structure is therefore based on the a face-centered cubic Bravais lattice with eight atoms per unit cell, as shown in Fig. 6.7a.

The crystal structure of Si is diamond cubic with a lattice parameter a of 0.543 nm at room temperature. Other group IVB elements, such as Ge and Sn (gray tin), also have the diamond structure. These elements have four outer-shell electrons, readily available to share electrons with four neighboring atoms, resulting in highly directional covalent bonds (Fig. 6.7b). The number of atoms/unit cells of the diamond lattice is given by $N_i = 4$, $N_f = 6$, and $N_c = 8$, so that

$$N_u = 4 + \frac{6}{2} + \frac{8}{8} = 8 \text{ atoms/unit cell.} \quad (6.4b)$$

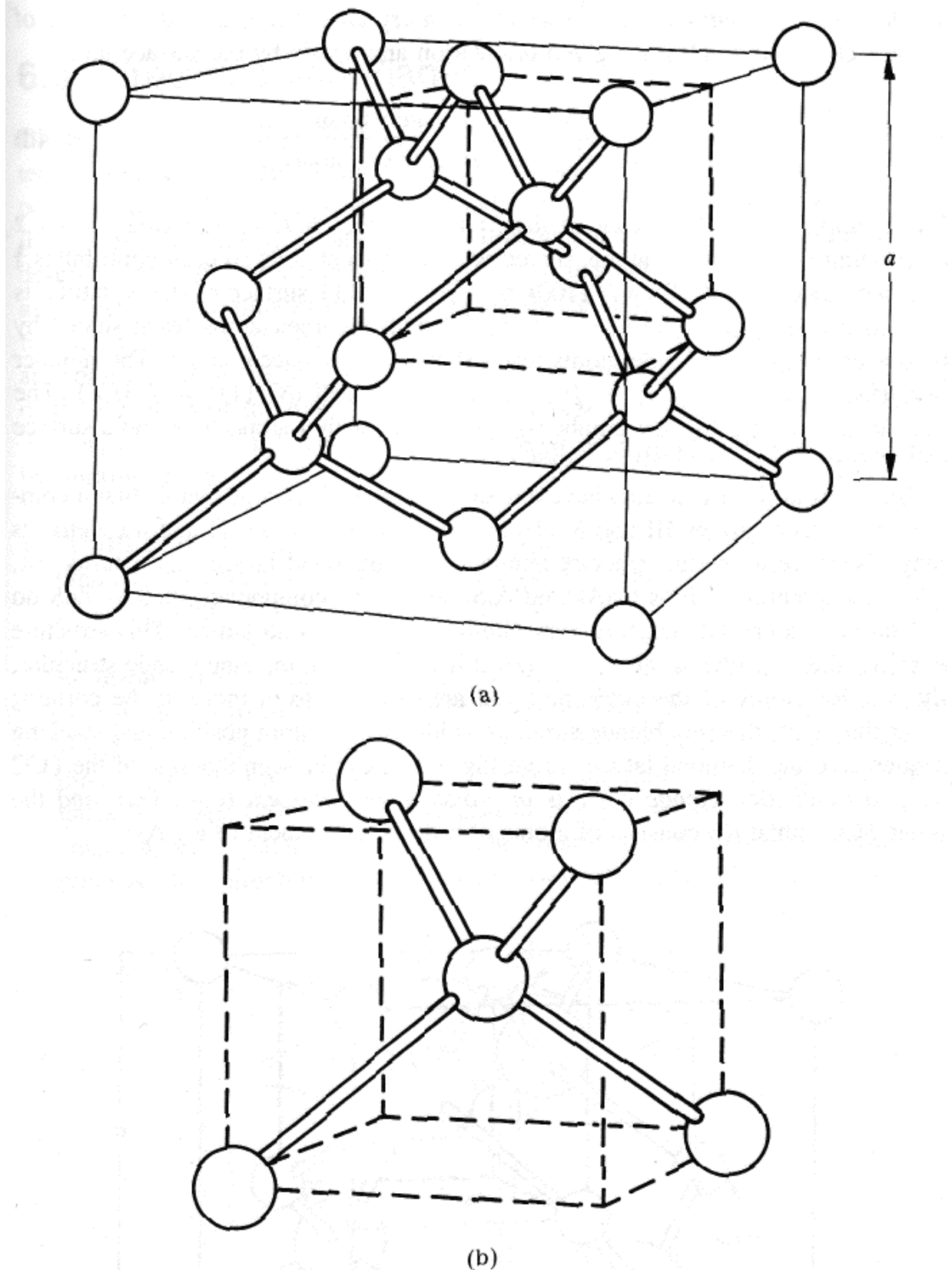


FIGURE 6.7 (a) Diamond lattice. The atoms are connected by covalent bonds. The cube outlined by the dashed lines shows one tetrahedral unit. (b) Tetrahedral unit of the diamond lattice.

The number of atoms/cm³, N , is given by

$$N = \frac{\text{atoms/unit cell}}{a^3}. \quad (6.4c)$$

To determine the number of atoms/cm² on a crystal surface, take the number of surface atoms/unit cell for a given orientation and divide by the surface area.

$$N'_s = \frac{\text{atoms}}{\text{cm}^2} = \frac{\text{surface atoms/unit cell}}{\text{surface cell area}}. \quad (6.4d)$$

For example, the 100 surface of the Si lattice, Fig. 6.7, has an area a^2 and 2 atoms/unit cell (4 corner atoms shared with 4 adjacent cells so each contributes $\frac{1}{4}$ and one center atom). Then $N'_s(100) = 2/a^2$. The 111 surface of the Si lattice is a triangle of length $a\sqrt{2}$ (area = $\sqrt{3}a^2/2$) with 3 corner atoms (each shared by 6 adjacent cells) and 3 side atoms (each shared by 2 adjacent cells). The number of surface atoms/cell is $(\frac{3}{6} + \frac{3}{2}) = 2$ atoms/unit cell ($N'_s(111) = 2.3/a^2$). The 110 surface has the highest number of atoms/cm² with 4 atoms/cell and a surface cell area of $\sqrt{2}a^2$ ($N'_s(110) = 2.8/a^2$).

Since group IVB elements have a diamond lattice, it is conceivable that a compound between groups III and V elements or between groups II and VI elements may also have a crystal structure similar to the diamond lattice. As it turns out, III–V compounds such as GaAs and AlSb and II–VI compounds such as ZnS do indeed have a crystal structure very similar to the diamond lattice. This structure is called the zinc blende structure, shown in Fig. 6.8. In the zinc blende structure, the interior atoms of the cubic unit cell are different from those at the corners; other than that, the zinc blende structure is identical in atom position and stacking sequence to the diamond lattice. From Fig. 6.8 it can be seen that one of the FCC sublattices of zinc blende consists of atoms of one element (e.g., Ga), and the other FCC sublattice consists of atoms of a different element (e.g., As).

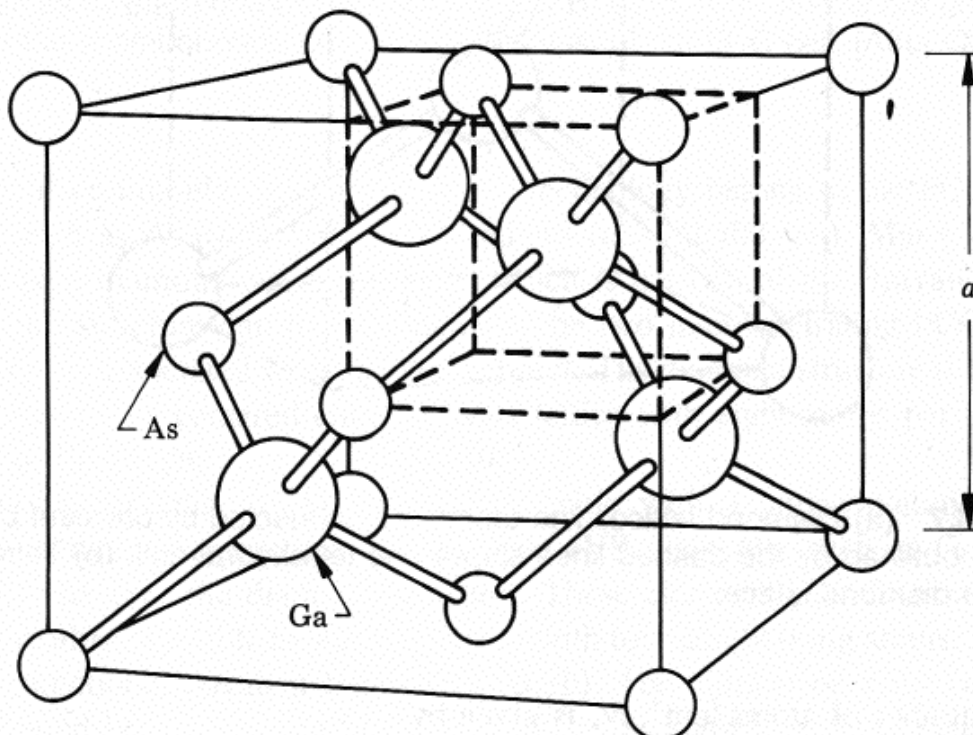


FIGURE 6.8 Zinc blende structure, showing Ga and As atoms.

6.3 Directions and Planes

Given a unit cell, the position of any lattice point in a cell may be described in terms of its coordinates; if the vector for the origin of the unit cell to the given point is $x\mathbf{a} + y\mathbf{b} + z\mathbf{c}$, where x , y , and z are fractions, then the coordinates of the given point are x , y , and z . The direction of any line in a lattice may be described by drawing a line through the origin parallel to the given line and then assigning the coordinates of any point on the line. Let's say that the line goes through the origin and the point with coordinates u , v , w , where these numbers are not necessarily integers. The direction $[uvw]$, written in brackets, are the indices of the direction of the line. Since this line also goes through $2u$, $2v$, $2w$ and $3u$, $3v$, $3w$, and so on, it is customary to convert u , v , w to a set of smallest integers by multiplication.

EXAMPLE 1

Find the coordinates of points A, B, C, and D and the directions of the lines going through them in Fig. 6.9.

Solution: We can define point A as the origin of the lattice; therefore, the coordinates of point A is 000. Point B has the coordinates of $1 \frac{1}{2} 0$, since point B can be brought from point A, the origin, by a vector $1\mathbf{a} + \frac{1}{2}\mathbf{b} + 0\mathbf{c}$. The direction of the line AB is $[1 \frac{1}{2} 0]$, or more conventionally, $[210]$. The coordinates of C are 100, and the direction of line AC is $[100]$, which is also the vector \mathbf{a} , the crystallographic axis. The coordinates of D are $\frac{1}{3} 1 1$, relative to point A. The direction of the line CD, however, is not $[133]$. Had a line been

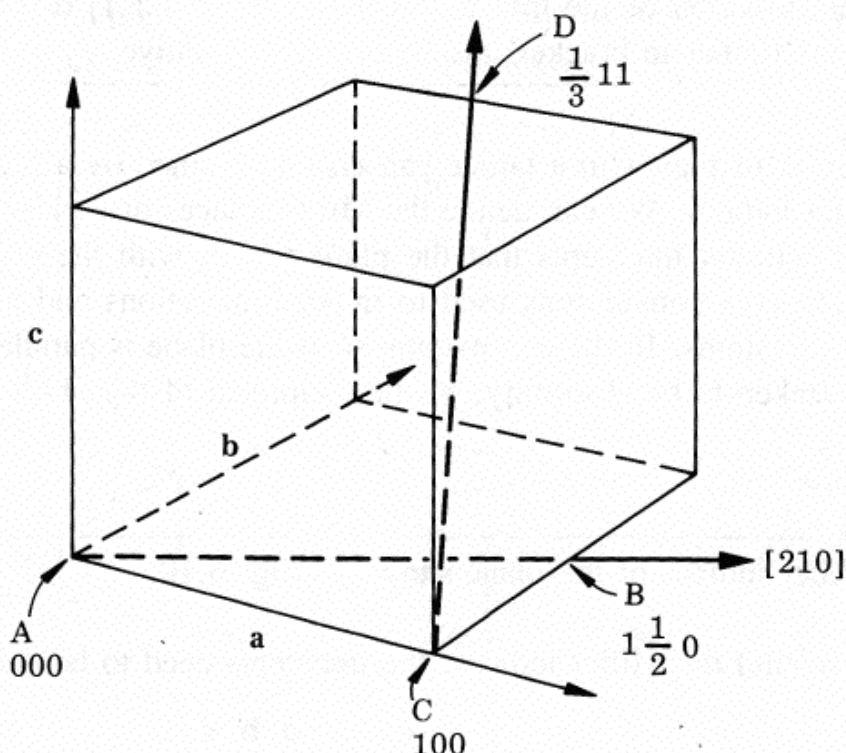


FIGURE 6.9 Directions and coordinates

TABLE 6.1 Conventions Used to Indicate Directions and Planes in Crystallographic Systems

- A. Directions: Line from origin to point at u, v, w
1. Specific directions are given in brackets, $[uvw]$.
 2. Indices uvw are the set of smallest integers.
 $[\frac{1}{2} \frac{1}{2} 1]$ goes to $[112]$.
 3. Negative indices are written with a bar, $[\bar{uvw}]$.
 4. Directions related by symmetry are given by $\langle uvw \rangle$.
 $[111], [\bar{1}\bar{1}1]$, and $[\bar{1}1\bar{1}]$ are all represented by $\langle 111 \rangle$.
- B. Planes: Plane that intercepts axes at $1/h, 1/k, 1/l$
1. Orientation is given by parentheses, (hkl) .
 2. hkl are Miller indices.
 3. Negative indices are written with a bar, (\bar{hkl}) .
 4. Planes related by symmetry are given by $\{hkl\}$.
 $(100), (010)$, and (001) are planes of the form $\{100\}$.
- C. In cubic systems: bcc, fcc, diamond
1. Direction $[hkl]$ is perpendicular to plane (hkl) .
 2. Interplanar spacing: $d_{hkl} = a/\sqrt{h^2 + k^2 + l^2}$.

drawn between A and D, the direction of the line AD would be $[133]$. The line CD is drawn between C and D; the direction indices must therefore be modified accordingly. This can be done by drawing a line from A parallel to the line CD. An equivalent operation would be to shift the origin from A to C. The coordinates of D relative to C are $-\frac{2}{3} 1 1$; this can be seen by traveling from C to D via the three crystallographic axes. Note that the direction of the line CA is $[\bar{1} 0 0]$. The direction of the line CD is therefore $[-\frac{2}{3} 1 1]$ or $[\bar{2}33]$. The bar on top of the number in brackets means that it is negative.

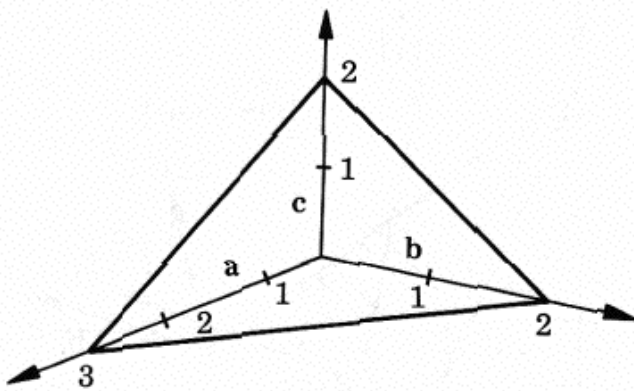
The orientation of planes in a lattice can also be defined by a set of numbers, called the Miller indices. We can define the Miller indices of a plane as the reciprocals of the fractional intercepts that the plane makes with the crystallographic axes. Table 6.1 gives conventions used to indicate directions and planes used in crystallographic systems. In these conventions, if the plane is parallel to the axis, the intercept is taken to be at infinity, ∞ ; the reciprocal of ∞ is $1/\infty = 0$.

EXAMPLE 2

Find the Miller indices of the plane shown in Fig. 6.10.

Solution: To find the Miller indices, the intercepts need to be defined.

	a	b	c
The intercepts	3	2	2
The reciprocals	$\frac{1}{3}$	$\frac{1}{2}$	$\frac{1}{2}$

**FIGURE 6.10** Plane in a lattice.The Miller indices $(\frac{1}{3} \frac{1}{2} \frac{1}{2})$

or

(multiply by 6) $(2 \ 3 \ 3)$

Figure 6.11 shows the Miller indices of some lattice planes. The planes are conventionally written as (hkl) and directions as $[uvw]$. For the cubic system, the direction $[hkl]$ is perpendicular to the plane (hkl) . The plane (hkl) is parallel to the $(\bar{h}\bar{k}\bar{l})$ plane, which is on the opposite side of the origin (see Table 6.1).

The dot product of $(hkl) \cdot [uvw]$ is the sum: $hu + kv + lw$. If the dot product of $(hkl) \cdot [uvw] = 0$, the direction $[uvw]$ lies on the plane (hkl) .

EXAMPLE 3

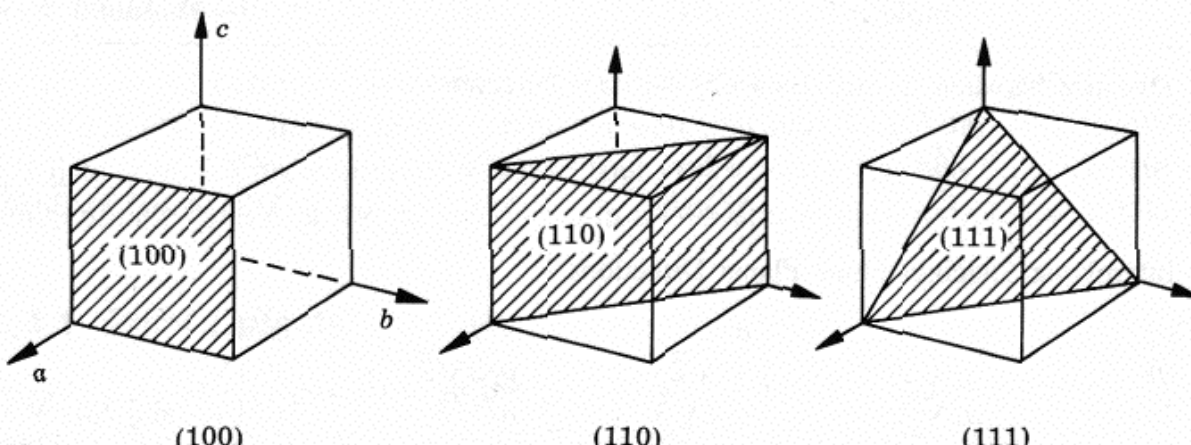
Determine if the plane (111) contains the following directions: $[100]$, $[\bar{2}11]$, and $[\bar{1}10]$.

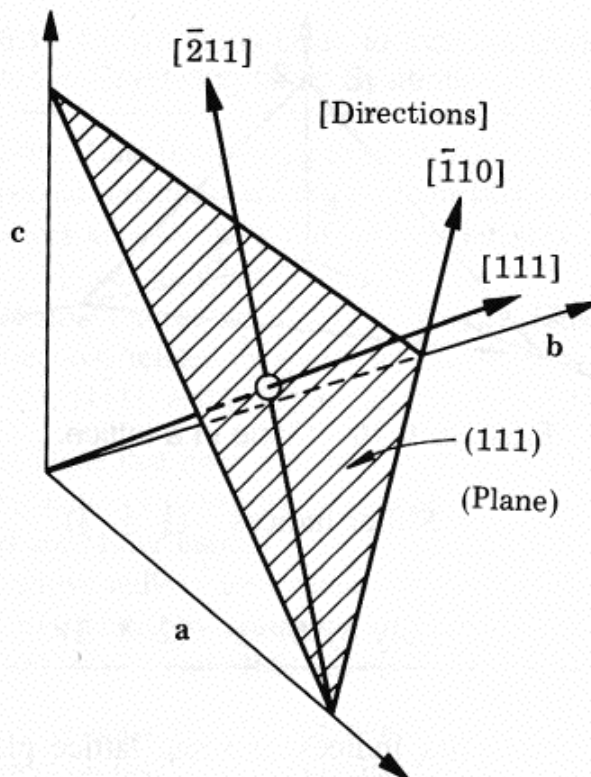
Solution: If the plane contains a direction, that direction should lie on the given plane. To check this, we take the dot products:

$$(111) \cdot [100] = 1 \quad [100] \text{ does not lie on } (111)$$

$$(111) \cdot [\bar{2}11] = 0 \quad [\bar{2}11] \text{ lies on } (111)$$

$$(111) \cdot [\bar{1}10] = 0 \quad [\bar{1}10] \text{ lies on } (111)$$

**FIGURE 6.11** Miller indices of lattice planes.

**FIGURE 6.12** The (111) plane.**EXAMPLE 4**

Show that the $[111]$ direction is perpendicular to the (111) plane (Fig. 6.12).

Solution: From Example 3 we know that $[\bar{2}11]$ and $[\bar{1}10]$ lie on (111) . Since both of these two vectors are perpendicular to the $[111]$ vector (the dot products are zero), the $[111]$ direction must be perpendicular to the (111) plane.

Table 6.2 gives distances between atoms and planes in the cubic system and Fig. 6.13 shows the lattice configuration for the zinc blende structure containing A and B atoms. With the knowledge of crystallography summarized above and in

TABLE 6.2 Distances Between Atoms and Planes in the Cubic System with Lattice Parameter a , Atomic Density N , and Number N_u of Atoms per Unit Cell

	Simple	bcc	fcc	Diamond
A. Distance between Atoms along Crystal Axis Directions				
$\langle 100 \rangle$	a	a	a	a
$\langle 110 \rangle$	$\sqrt{2}a$	$\sqrt{2}a$	$a/\sqrt{2}$	$a/\sqrt{2}$
$\langle 111 \rangle$	$\sqrt{3}a$	$\sqrt{3}a/2$	$\sqrt{3}a$	$\sqrt{3}a/4$ and $3\sqrt{3}a/4$
B. Interplanar Spacings along Planar Directions				
$\{100\}$	a	$a/2$	$a/2$	$a/4$
$\{110\}$	$a/\sqrt{2}$	$a/\sqrt{2}$	$a/2\sqrt{2}$	$a/2\sqrt{2}$
$\{111\}$	$a/\sqrt{3}$	$a/2\sqrt{3}$	$a/\sqrt{3}$	$a/4\sqrt{3}$ and $3a/4\sqrt{3}$

$$N = N_u/a^3 \text{ with } N_u = 1, 2, 4, \text{ and } 8 \text{ for simple cubic, bcc, fcc, and diamond lattices, respectively.}$$

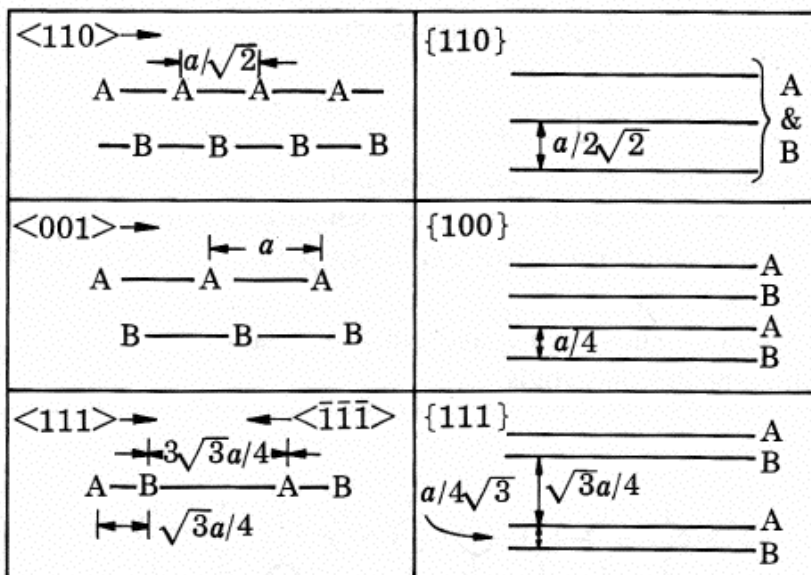


FIGURE 6.13 Lattice configuration for the zinc blende lattice with a as the lattice constant with A and B denoting Ga and As atoms in GaAs.

Fig. 6.8, it can be seen that the zinc blende unit cell (using GaAs as an example) can be generated by constructing a Ga FCC sublattice with the origin assigned at 000, followed by constructing an As FCC sublattice with an origin at $\frac{1}{4}\frac{1}{4}\frac{1}{4}$ of the Ga sublattice. It can also be seen in Fig. 6.13 that the atomic layer sequence viewed along the [111] direction is different from that viewed along the [$\bar{1}\bar{1}\bar{1}$] direction. This variation in sequences causes significantly different surface properties between the (111) surface and the ($\bar{1}\bar{1}\bar{1}$) surfaces, referred to as A and B faces. The (111) Ga face (A face) has gallium atoms with no free electrons. The ($\bar{1}\bar{1}\bar{1}$) As face [sometimes it is just called the (111) As face without the bars, the B face] consists of arsenic atoms with two free electrons (Ghandhi, 1983). The (111) As face is thus electronically more active than the (111) Ga face. Etching of the (111) As face occurs very rapidly, with a resultant smooth polish. The (111) Ga face etches very slowly, so that all imperfections become delineated. The (111) As face oxidizes more readily and has a higher As vapor pressure ($T < 770^\circ\text{C}$) than the (111) Ga face.

6.4 Crystalline Defects

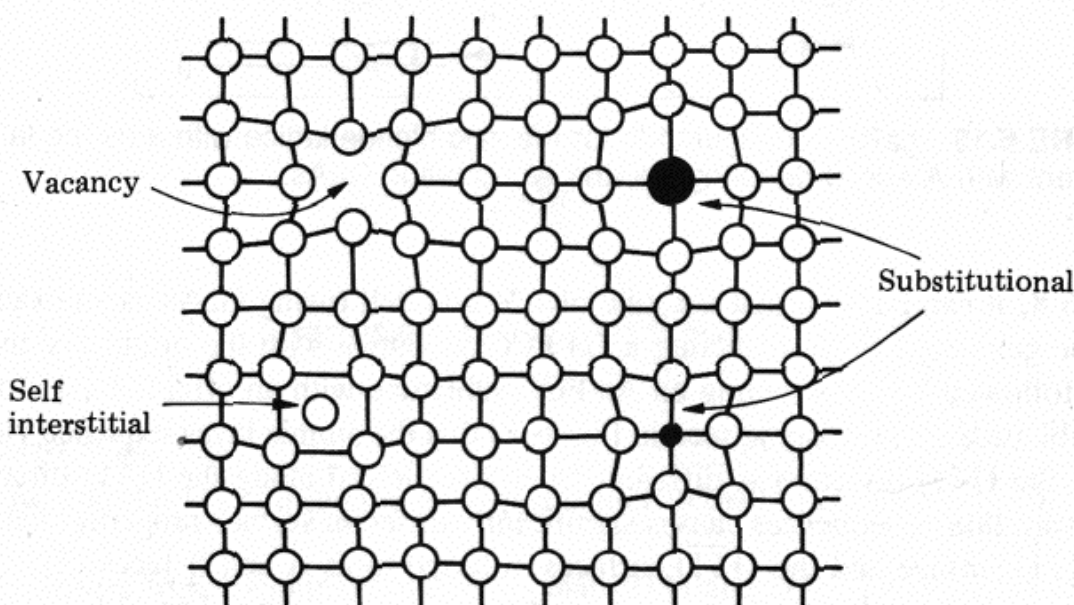
As mentioned before, defects in a crystalline material may be categorized as (1) point defects, (2) line defects, (3) planar defects, and (4) volume defects. Table 6.3 lists some of the examples of these four types of defects, and Fig. 6.14 shows schematically some of the point defects in a two-dimensional simple cubic lattice.

6.4.1 Point Defects

A point defect is a deviation in the periodicity of the lattice arising from a single point. Other defects, such as dislocations and stacking faults, extend over many lattice sites. Point defects may exist as a result of thermal equilibrium, whereas

TABLE 6.3 Crystalline Defects in Semiconductors

Defect Type	Examples
Point	Vacancies, interstitials, impurity atoms, antisite defects, extended point defects [not as localized as a simple point defect (e.g., an interstitial atom can form a defect complex with one or more neighboring atoms)]
Line	Dislocations
Plane	Stacking faults, twins, and grain boundaries
Volume	Precipitates and voids

**FIGURE 6.14** Various points defects in a simple cubic lattice.

other types of defects form due to nonequilibrium conditions such as occur during crystal growth or during thermal or mechanical processing of the material. Point defects may be categorized as (1) native defects such as a vacancy, and (2) impurity-related defects due to the introduction of an impurity atom into the lattice. For semiconductors, point defects not only cause structural disturbances, but also often introduce electronic states in the band gap. If an attractive potential exists between a native defect and an impurity atom, they may interact and form a defect complex, such as a vacancy–impurity pair.

6.4.2 Native Defects and Shallow Dopants

For Si, there are three types of native defects: the vacancy, the interstitial, and the interstitialcy. The vacancy is an empty lattice site, referred to as V in the literature. Depending on the configuration of the unsatisfied bonds due to the missing atom, a vacancy in Si can be either neutral or negatively or positively charged. A vacancy is also referred to as a Schottky defect. A Si atom residing in the interstices of the Si lattice is defined as a self-interstitial. A Frenkel pair is a vacancy–interstitial pair formed when an atom is displaced from a lattice site to an interstitial site. An

interstitialcy consists of two atoms in nonsubstitutional positions configured about a single lattice site. Because of the similarity between an interstitial and an interstitialcy, a distinction is generally not made; both are identified as I in the literature. When an impurity such as a shallow dopant (e.g., As in Si) occupies a lattice site, it is known as a substitutional defect. Such a defect when surrounded only by Si atoms on their normal sites is identified as A . When a vacancy V forms next to A , it is known as an impurity vacancy pair, usually referred to as an AV defect. If one of the atoms in the interstitialcy defect is a dopant atom, the defect is referred to as an AI defect. If the impurity atom occupies an interstitial site, it is designated as A_i ; if the impurity atom occupies a substitutional site, it is designated as A_s .

For GaAs and other III–V compounds and alloys, it should be noted that defects may occupy lattice sites either in the Ga (group III) sublattice or in the As (group V) sublattice or both. For example, an empty As lattice site is referred to as the V_{As} defect. A Si atom occupying a Ga site is referred to as the Si_{Ga} defect. Since Si is a group IV element substituting for Ga, a group III element, this Si_{Ga} defect is an n -type dopant. A Si atom occupying an As site is referred to as a Si_{As} defect, which is a p -type dopant for GaAs. For Si atoms diffused into GaAs, or implanted Si atoms after thermal activation, the Si atoms tend to occupy the sites in the Ga sublattice preferentially. As a result of the concentration of Si_{Ga} being greater than the concentration of Si_{As} , Si is generally an n -type dopant for GaAs and its alloys. It has been observed that Ge behaves similarly to Si, but carbon is found to be an acceptor in GaAs. When the concentration of Si_{As} becomes comparable to that of Si_{Ga} , the semiconductor is said to have been compensated and the electrical conductivity of the semiconductor decreases. It is also possible for a Ga atom to be located on an As site, Ga_{As} , or an As atom on a Ga site, As_{Ga} . These defects are called antisite defects. It has been suggested that the commonly observed deep-level donor center, EL2, in GaAs is due to the antisite defect As_{Ga} (Lagowski et al., 1982; Kirkpatrick et al., 1985). The other antisite defect, Ga_{As} , is believed to be a double acceptor (i.e., can trap two holes).

6.4.3 Thermodynamics of Point Defects

Native point defects exist under thermodynamic equilibrium conditions due to the increase in configurational entropy of the crystal which their presence creates. This can be seen by considering the configurational entropy of mixing between vacancies and atoms in a lattice starting from the Boltzmann expression of entropy:

$$S = k \ln W, \quad (6.5)$$

where S is the entropy, W the number of ways for arranging the defects in a crystal, and k the Boltzmann factor. Assuming that there are n vacancies in a crystal of N lattice sites, we obtain

$$\begin{aligned} W &= \frac{N(N - 1) \cdots (N - n + 1)}{n!} \\ &= \frac{N!}{(N - n)! n!}. \end{aligned} \quad (6.6)$$

Using the Stirling's approximation of $\ln x! \approx x \ln x; x \rightarrow \text{large}$

$$S = k [N \ln N - (N - n) \ln (N - n) - n \ln n]. \quad (6.7)$$

The free energy of a system is

$$G = H - TS \quad (6.8)$$

where G is the Gibbs free energy, H the enthalpy, T the absolute temperature, and S the entropy. The change of the free energy of the lattice due to the presence of the vacancies is

$$\Delta G = nH_v^f - T(S + nS_v^f) \quad (6.9)$$

where H_v^f is the enthalpy of formation of a vacancy and S_v^f is the vibrational entropy, which is generally small compared to S [eq. (6.5)]. Under thermodynamic equilibrium,

$$\frac{\partial \Delta G}{\partial n} = 0. \quad (6.10)$$

From eq. (6.9) we have

$$\frac{\partial \Delta G}{\partial n} = H_v^f - TS_v^f - T \frac{\partial S}{\partial n} = 0. \quad (6.11)$$

From eq. (6.7) we have

$$\frac{\partial S}{\partial n} = k \ln \frac{N - n}{n}.$$

Substituting into eq. (6.11) yields

$$H_v^f - TS_v^f - kT \ln \frac{N - n}{n} = 0$$

or

$$\frac{n}{N - n} = \exp \left(\frac{S_v^f}{k} \right) \exp \left(- \frac{H_v^f}{kT} \right). \quad (6.12)$$

Since $N \gg n$, eq. (6.12) may be written as

$$\frac{n}{N} = \exp \left(\frac{S_v^f}{k} \right) \exp \left(- \frac{H_v^f}{kT} \right). \quad (6.13)$$

The derivation above is for uncharged vacancies (neutral vacancies); therefore, the neutral vacancy concentration $[V^x]$ is

$$[V^x] = N \exp \left(\frac{S_v^f}{k} \right) \exp \left(- \frac{H_v^f}{kT} \right). \quad (6.14)$$

We use the bracket notation to indicate concentrations. For metals, H_v^f is between 0.5 and 1 eV. The rule of thumb is: $H_v^f \approx 10kT_m$ (T_m = melting point in K). For

Si, $H_v^f \approx 2.4$ eV and for Ge, $H_v^f \approx 2.2$ eV. The term $\exp(S_v^f/k)$ is of the order of 1. [$S_v^f \approx 1.1 k$ for Si, so that $\exp(1.1)$ is a factor of 3.] The equilibrium concentration of neutral vacancies in silicon is independent of the position of the Fermi level, and with $N = 5.0 \times 10^{22}/\text{cm}^3$ (the concentration of Si lattice sites),

$$[V^x] = 5.0 \times 10^{22} \times 3 \times e^{-2.4/kT} = 1.5 \times 10^{23} e^{-2.4/kT} \quad (6.14a)$$

$= 1.3 \times 10^{13}/\text{cm}^3$ at 1200 K.

There is a major difference between defects (vacancies and interstitials) in semiconductors and those in metals; that is, defects in a semiconductor can be charged electrically, whereas defects in a metal are considered neutral. Since defects can be charged (or ionized), the concentration of these defects becomes a function of the Fermi level position in the semiconductor. Let us use the charged states of vacancies in Si as an example. It is generally accepted that the single vacancy in Si can have four charge states (Van Vechten, 1980): V^+ , V^x , V^- , and $V^=$, where $+$ refers to a donor state, x a neutral species, and $-$ an acceptor state. Figure 6.15 shows the energy levels of the charged vacancies in the Si band gap at 0 and 1400 K, V^+ state has an energy level E^+ , V^- has an energy level E^- , and so on. These energy levels are estimated values but are sufficiently accurate for demonstration purposes.

The concentration of charged vacancies is governed by the Fermi–Dirac statistics (see Chapter 12) and is given by (using V^- as an example)

$$[V^-] = \frac{[V_T]}{1 + e^{(E^- - E_F)/kT}} \quad (6.15)$$

where E_F is the Fermi level, E^- is the energy level of the acceptor state vacancy, and $[V_T]$ is the total vacancy concentration:

$$[V_T] = [V^x] + [V^-] + [V^=] + [V^+]. \quad (6.16)$$

After some algebraic manipulation of eqs. (6.15) and (6.16) (see the problems) we find that

$$[V^-] = [V^x] \exp[(E_F - E^-)/kT] \quad (6.17)$$

and similarly,

$$[V^+] = [V^x] \exp[(E^+ - E_F)/kT]. \quad (6.18)$$

Upon examining eq. (6.17), we find that the concentration $[V^-]$ is large compared to $[V^x]$ only when $(E_F - E^-) \gg kT$ and positive. This means that $[V^-]$ is significant when the Si sample is strongly *n*-type (i.e., E_F is located far above E^-).

As the Si sample becomes less *n*-type and E_F goes below E^- , $[V^-]$ decreases accordingly. For *p*-type samples where E_F is far below E^- , $[V^-]$ is negligible small compared to $[V^x]$. Figure 6.16 shows the graphical representation of $[V^-]$, $[V^=]$, and $[V^+]$ as a function of the Fermi level E_F for two temperatures. According to eq. (6.18) and Fig. 6.16, the concentration $[V^+]$ is large compared to $[V^x]$ when E_F is located far below E^+ (i.e., strongly *p*-type). $[V^+]$ becomes negligibly small for *n*-type Si.

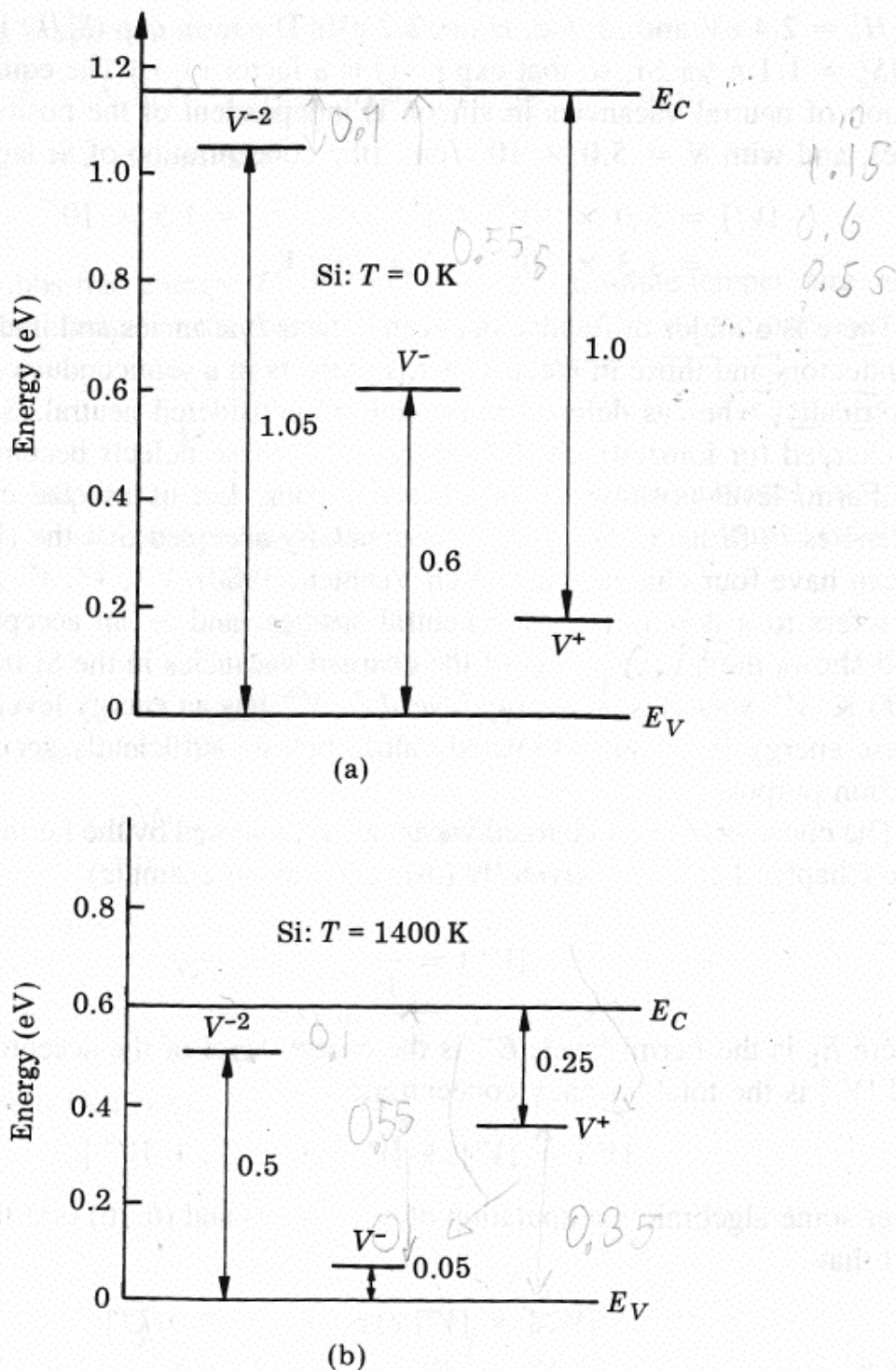


FIGURE 6.15 Energy levels of vacancies of Si at (a) 0 K and (b) 1400 K. [After Van Vechten (1980).]

EXAMPLE 5

Calculate the concentration $[V^-]$ at 1400 K in an *n*-type Si doped with a donor density of $2.8 \times 10^{20}/\text{cm}^3$.

Solution: We start by calculating the Fermi level of this sample at 1400 K. From eq. (3.10) we have

$$E_F = E_C + kT \ln \frac{n}{N_C}$$

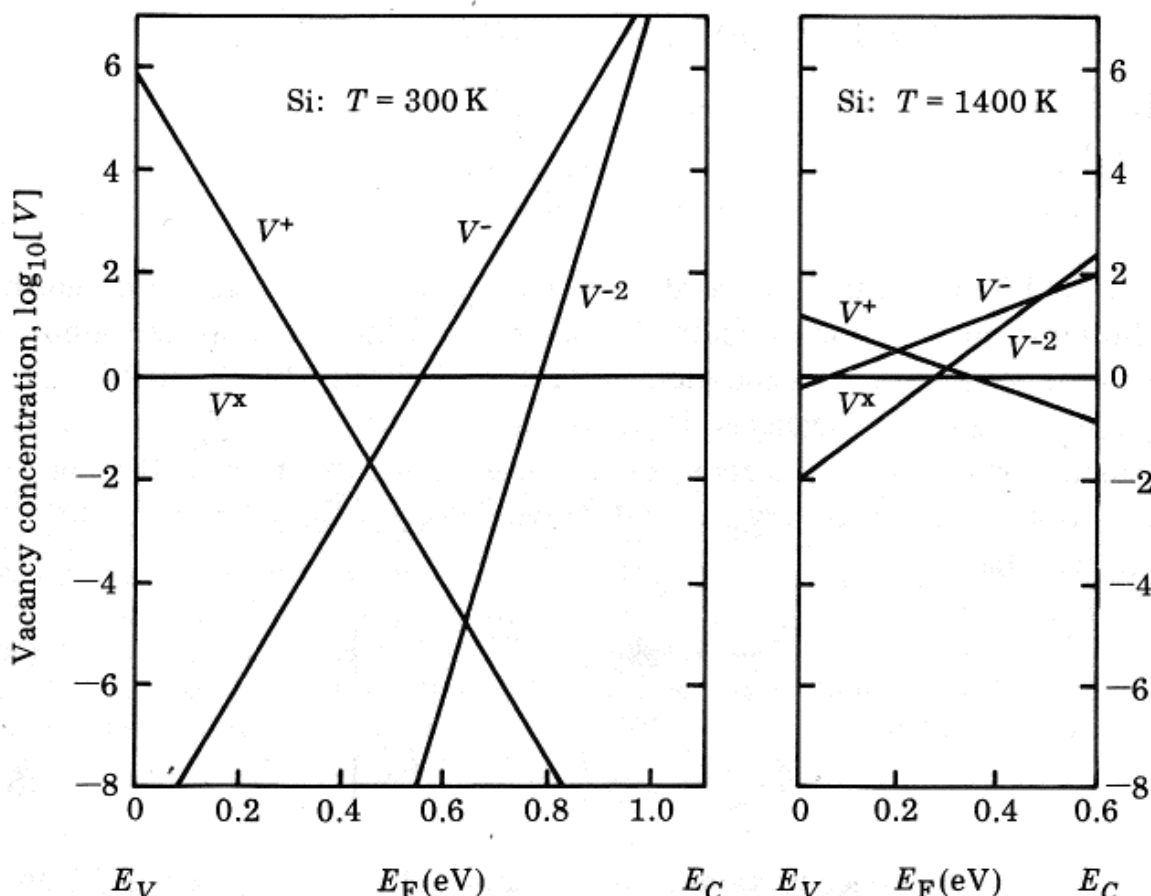


FIGURE 6.16 Variation of the relative concentration of charged states of the single Si vacancy with position of E_F at two temperatures. [After Van Vechten (1980).]

The value of n is taken to be the donor density ($2.8 \times 10^{20}/\text{cm}^3$). The value of N_C at 1400 K can be calculated using eq. (3.6) and Table 3.3:

$$N_C(1400 \text{ K}) = \frac{N_C(300 \text{ K})(1400)^{3/2}}{(300)^{3/2}} = 2.8 \times 10^{20} \text{ cm}^{-3}$$

We see that N_C is just equal to N_D . We may then take E_F to be located at E_C as suggested by eq. (3.10).

At 1400 K, the band gap of Si is reduced from 1.15 eV at 300 K to 0.6 eV at 1400 K (Van Vechten, 1980). The energy level of E^- tracks the band gap and is located at 0.05 eV + E_V at 1400 K (Fig. 6.15). The concentration $[V^-]$ is given by eq. (6.17):

$$\begin{aligned}[V^-] &= [V^x] \exp\left(\frac{E_F - E^-}{kT}\right) = [V^x] \exp\left(\frac{E_C - 0.05 - E_V}{kT}\right) \\ &= [V^x] \exp\left(\frac{E_G - 0.05}{kT}\right) = [V^x] \exp\left(\frac{0.55}{0.12}\right) \\ &= 98[V^x].\end{aligned}$$

Therefore, $[V^-]$ is about 100 times higher than $[V^x]$ at 1400 K, in agreement with the result shown in Fig. 6.16. The equilibrium concentration of neutral vacancy $[V^x]$ at 1400 K is

$$[V^x] = 1.5 \times 10^{23} \exp(-2.4/kT) = 3.4 \times 10^{14}/\text{cm}^3.$$

Therefore,

$$[V^-] = 3.3 \times 10^{16}/\text{cm}^3.$$

It should be noted that the creation of ionized vacancies does not diminish the equilibrium concentration of neutral vacancies $[V^x]$. More neutrals are simply created to maintain their concentration at the level indicated by eq. (6.14), and the total concentration of vacancies, $[V_T]$, increases accordingly.

Generalizing from the vacancy concentrations [eqs. (6.14) to (6.18)], the equilibrium concentrations of any charged native defect, X , may be related to that of the neutral state:

$$\frac{[C_x^-]}{[C_x^0]} = \exp\left(-\frac{E_x^- - E_F}{kT}\right) \quad (6.19)$$

$$\frac{[C_x^+]}{[C_x^0]} = \exp\left(-\frac{E_F - E_x^+}{kT}\right) \quad (6.20)$$

where $[C_x^0]$ is the concentration of the neutral defects, $[C_x^-]$ and $[C_x^+]$ are the concentrations of the charged defects with energy level E_x^- and E_x^+ , respectively, and E_F the Fermi level. Equations (6.19) and (6.20) are general for dilute doping concentrations. If the charged defects are vacancies, eqs. (6.19) and (6.20) reduce to eqs. (6.17) and (6.18). When the doping concentration increases to high concentrations such that dopant–dopant and dopant–defect interactions cannot be ignored, these equations may no longer hold. **Point defects play very significant roles in solid-state diffusional processes** and the issues are addressed in Chapter 7.

6.4.4 Deep Level Centers

Shallow dopant impurities have small ionization energies (such as As and P in Si with ionization energies of ~ 0.04 eV). There are chemical impurities and charged point defects that form deep energy states in semiconductors. The energy levels of these centers in the band gap are usually far away from the band edges; thus they are called deep level centers. Typical deep level impurities are oxygen and metallic elements in Si and in GaAs. A deep level impurity may have several energy levels, with each energy level being either an acceptor state or a donor state. For example, Au and Si has an acceptor state at 0.54 eV from the conduction band edge, E_C , and a donor state 0.35 eV from the valence band edge, E_V (Fig. 6.17). Other than chemical impurities, charged point defects such as V^- in Si, and V_{Ga} and antisite defects in GaAs, also form deep level states. It should be noted that there are many deep levels centers in III–V compounds and alloys whose physical origins have not been clearly identified. A typical example is the DX center in AlGaAs. These centers are found to be deep donors of unknown origin—therefore, DX centers.

A deep center may act either as a trap or as a recombination center, depending on the impurity, temperature, and other doping conditions. Consider a minority

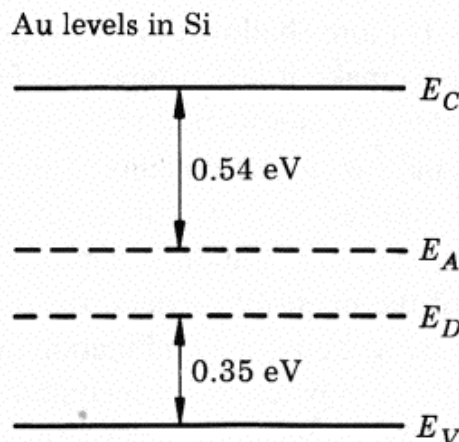


FIGURE 6.17 Au in Si has an acceptor state, E_A ($\approx E_C - 0.54$ eV) and a donor state, E_D ($\approx E_V + 0.35$ eV). For strongly *p*-type Si, the Fermi level E_F is below E_D ; the donor states are ionized (the electron in the state is given away) and become positively charged. The acceptor state at E_A is not ionized (the state has not received an electron because E_F is far away below E_A). For strongly *n*-type Si, E_F is far above E_A ; the acceptor states are ionized (the state has received an electron) and become negatively charged. The Au donor states are not ionized in strongly *n*-type Si.

carrier (holes in an *n*-type semiconductor, for example) captured at an impurity center. The minority carrier stays at the center for a period of time and is then ejected thermally into the band from which it came; this impurity center is known as a trap. Before ejection, if a majority carrier is captured, recombination of the carrier pair takes place and the center is therefore a recombination center.

For deep centers to be effective recombination centers, they should be (1) singly charged and attractive to the minority carriers and (2) neutral after the capture of a minority carrier. Capture of majority carriers by neutral centers is highly probable because of the large number of majority carriers. For the impurity centers to be effective traps, they should be (1) doubly charged and attractive to the minority carriers and (2) repulsive to the majority carriers, after capturing one minority carrier. Before capturing of majority carrier (not a very probable event because of the small capture cross section), the minority carrier is ejected. The capture efficiency of carriers by these impurities depends on the capture cross section, which is a measure of the probability of the capturing event. The cross section of attractive centers is $\approx 10^{-12}$ to 10^{-15} cm 2 , the cross section of neutral centers is $\approx 10^{-15}$ to 10^{-17} cm 2 , and the cross section of repulsive centers is $\approx 10^{-22}$ cm 2 .

As mentioned previously, Au can be either a deep acceptor or a deep donor in Si (Au can be neutral as well). These impurities are called amphoteric dopants. For example, substitutional In is a deep acceptor in Si, interstitial In in Si is a deep donor. Si in GaAs is a donor when occupying a vacant Ga site, and an acceptor when occupying a vacant As site. These elements can be either donors or acceptors, depending on their lattice location. Let's consider a Si wafer containing Au. In strongly *p*-type Si, Au donors are ionized and become positively charged, thus attractive to the minority carriers, that is, the electrons (Fig. 6.17). After the capture of an electron, the Au donor state becomes neutral and is now effective in capturing the majority carriers, the holes. The donor states of Au are, therefore, recombi-

nation centers in *p*-type Si. If more shallow dopants (phosphorus, for example) are introduced into this sample to make it less *p*-type, the Fermi level will rise. As E_F crosses E_D , the Au donor states are not likely to be ionized and cease to be electron traps. Further increase in shallow *n*-type dopants causes E_F to rise above E_A . The Au acceptor states are now ionized and become negatively charged, thus effective in capturing holes. After capturing the minority carriers, the centers become neutral and ready for the capture of the majority carriers, the electrons. In strongly *n*-type Si, the Au acceptor states are effective recombination centers.

Since deep level impurities can be effective recombination centers, the presence of these defects may reduce the minority-carrier lifetime (see Section 3.8). A long minority-carrier lifetime is usually beneficial to device operations. It is sometimes necessary to reduce the amount of deep impurities by “gettering” processes.

The detection and characterization of deep level defects are difficult even for high-resolution electron microscopy (HREM). An experimental technique known as deep level transient spectroscopy (DLTS) has been developed to characterize these defects (Lang, 1974). One convenient way to perform DLTS is to measure the capacitance change of a sample when a pulse of charge is injected into the sample, normally under a reverse bias. From the change of the capacitance as a function of temperature, the defect density and defect energy level may be deduced.

6.5 Line Defects

Line defects in a crystalline material are known as dislocations. In contrast to point defects, dislocations are formed due to nonequilibrium conditions such as thermal and mechanical processing and epitaxy. Under equilibrium conditions, there is no requirement for the presence of dislocations or any other defects (except native point defects) in the crystal. For this reason it is possible to grow dislocation free single crystals of semiconductors. For example, Si wafers contain typically less than $100 \text{ dislocations/cm}^2$, compared to $10^8 \text{ dislocations/cm}^2$ or more in the metal interconnect lines on a chip. Chemical etching of the Si wafer reveals the dislocations at the surface in the form of small pits (Jenkins, 1977). The etch pit density (EPD) is used as a means to indicate wafer quality, with values less than $10^2/\text{cm}^2$ indicative of high quality. Defect etches are also used in GaAs (Stirland, 1988).

A dislocation may be created in the following manner in a simple cubic lattice (see Fig. 6.18): Make a cut on the crystal along any plane. Let the crystal on one side of cut shift by a vector parallel to the cut surface relative to the other half (along line AA in Fig. 6.18a). Then join the atoms on either side of the cut. A *screw* dislocation is thereby created (Fig. 6.18a). If the shift is perpendicular to the cut, an *edge* dislocation is created (Fig. 6.18b). If the shift is neither parallel nor perpendicular to the cut, the dislocation is called a *mixed* dislocation. An edge dislocation may be viewed also as having an extra half-plane inserted into the crystal (see Fig. 6.19). In addition to the edge, screw, and mixed dislocations, any dislocation may be either a perfect dislocation or an imperfect (or partial) dislocation. For a perfect dislocation the shift or translational vector connects identical

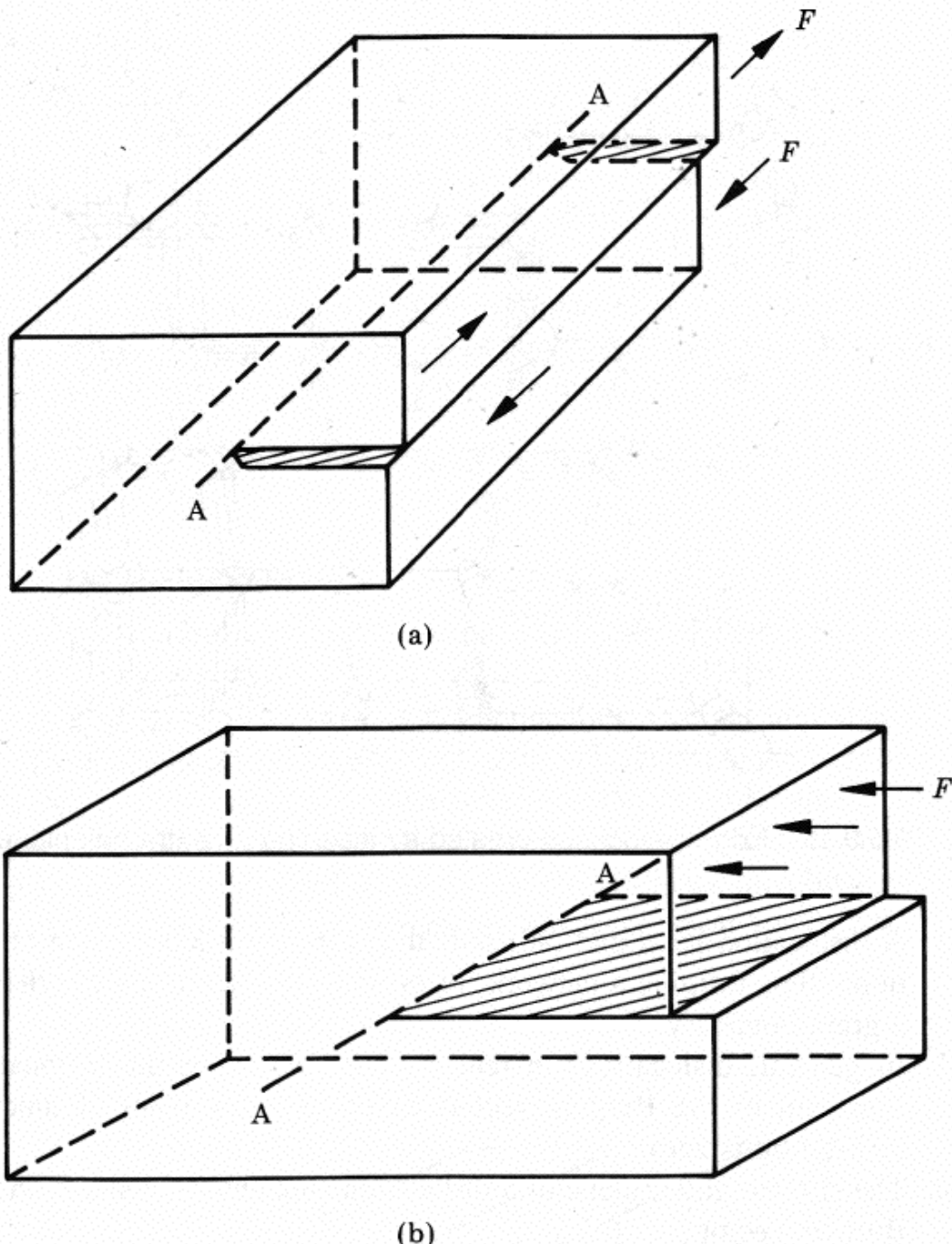


FIGURE 6.18 (a) Parallel shift to line AA—screw dislocation; (b) perpendicular shift to line AA—edge dislocation.

lattice points. For an imperfect (or partial) dislocation, the translational vector does not end on an identical lattice point.

The translational or shift vector of a dislocation is commonly known as a Burgers vector, **b**. The Burgers vector of an edge dislocation is readily determined by drawing a Burgers circuit around an edge dislocation. The Burgers vector **b** is perpendicular to the dislocation line for an edge dislocation (Fig. 6.20). For a screw dislocation, the Burgers vector **b** is parallel to the dislocation line.

Several properties of a dislocation should be noted (Read, 1953):

1. For a given dislocation, there is only one Burgers vector, no matter what shape the dislocation line has.

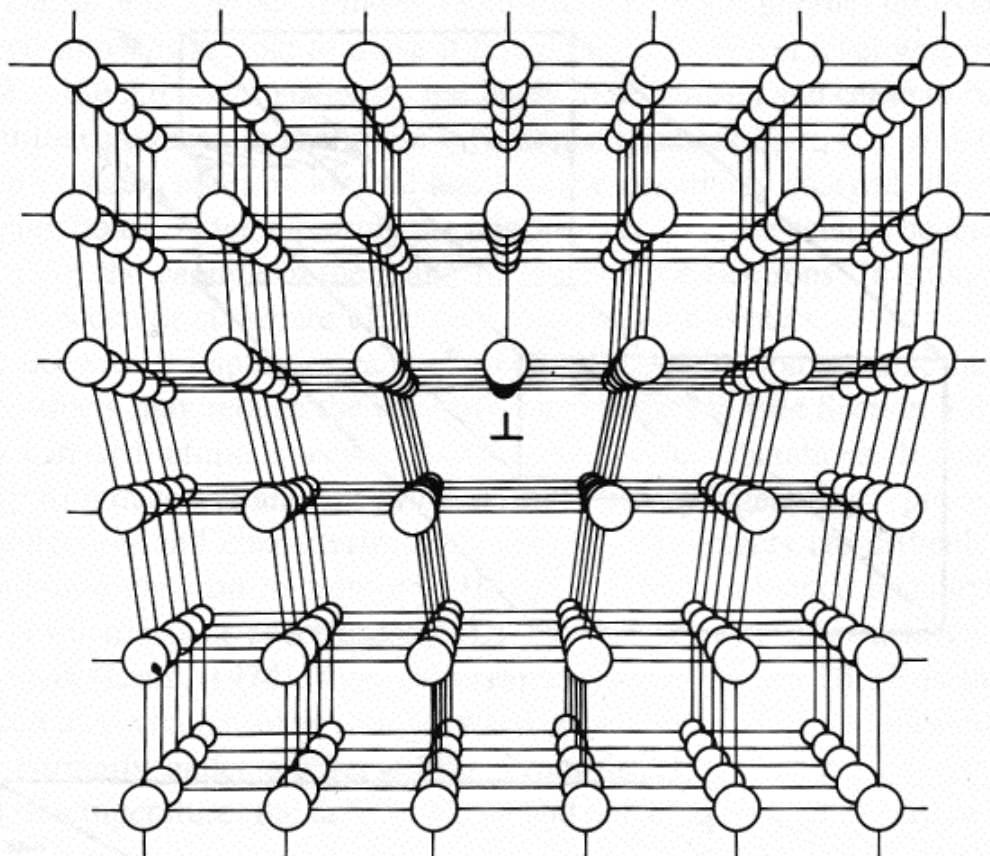


FIGURE 6.19 Edge dislocation created by inserting an extra half-plane of atoms.

2. A dislocation must end on itself, thus forming a loop, or on other dislocations, thus forming a network, or on surfaces such as an external surface or a grain boundary.
3. In general, dislocations in real crystals form three-dimensional networks. The sum of the Burgers vectors at the node or point of junction of the dislocation is zero.
4. The slip (or glide) plane of a dislocation contains the dislocation line and its Burgers vector.

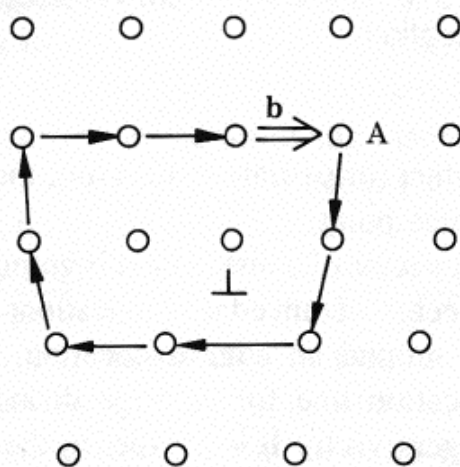


FIGURE 6.20 The Burgers vector of an edge dislocation is determined by drawing a Burgers circuit around a dislocation. Look along the dislocation (the symbol \perp represents a dislocation going into the plane of the page) and draw a circuit (starting from atom A) in the clockwise direction. The Burgers vector \mathbf{b} is the vector to close the circuit.

5. When a dislocation slips on its slip plane, the atoms move in the direction of the Burgers vector, but the dislocation line moves normal to itself on the slip plane.

Dislocations in diamond cubic and zinc blende lattice usually lie along $<110>$ directions due to the directionality of the bonds [the directionality is sometimes referred to as the Peierls force in a crystal; Hirth and Lothe (1968)]. The Burgers vector is of the $(a/2) <110>$ type (i.e., a Burgers vector with magnitude of $a/2$ directed along the $<110>$ direction). The dislocations in these crystals are therefore usually 60° mixed dislocations or screw dislocations. It should be pointed out that for III–V compounds the unbounded atoms at the dislocation may be on either the III or V element.

6.5.1 Force on Dislocations

Consider a crystal containing a single edge dislocation (Fig. 6.21). The crystal has a volume of $D \times l \times H$. In order for the edge dislocation to move, a shear stress must be applied to the crystal. Stresses are defined as force per unit area (N/m^2 ; $1 \text{ N/m}^2 = 10 \text{ dyn/cm}^2$). Shear stresses are due to forces applied tangentially to the surfaces. Normal stresses, on the other hand, are due to forces applied perpendicular to the surfaces. In Fig. 6.21 the shear forces are applied to the top and bottom surface of the crystal, resulting in a shear stress τ in the directions indicated by the arrows in the figure. The surfaces on which the shear forces are applied have an area of $D \times l$.

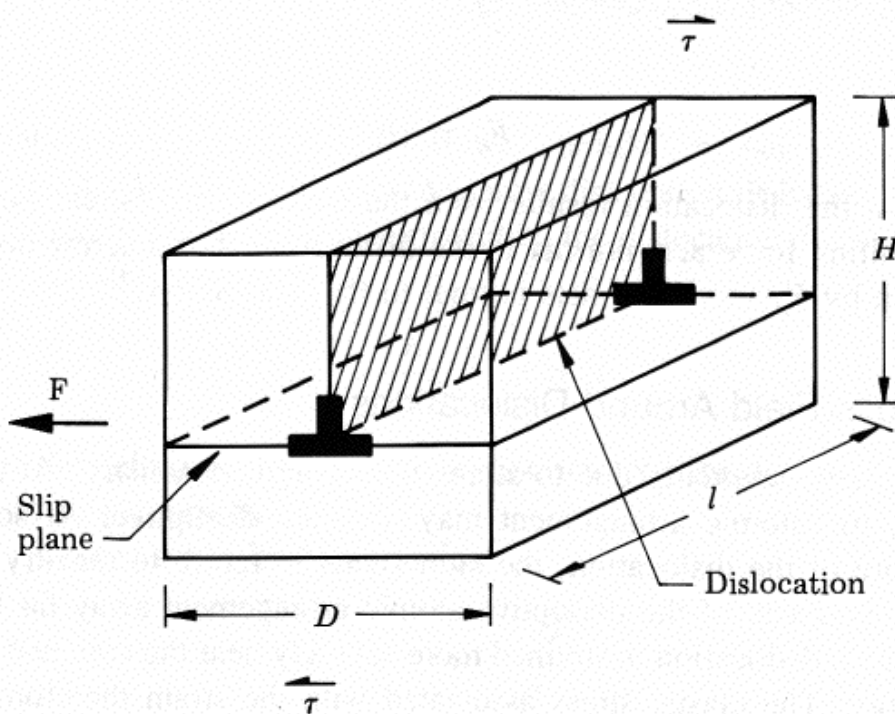


FIGURE 6.21 Edge dislocation contained in a crystal under an applied shear stress τ . The crystal has dimensions $D \times l \times H$. The dislocation with length l slips from the right-hand side of the crystal to the left-hand side of the crystal. This motion of the dislocation causes the crystal to slip by a distance b .

The work done by an applied shear stress τ which causes the crystal to slip by a distance b (the Burgers vector) is

$$W_\tau = \tau l D b \quad (6.21)$$

where W_τ is the work done by the applied shear stress, l the length of the edge dislocation, b the Burgers vector, and D the width of the crystal. The upper half of crystal slips by a distance b relative to the lower half of the crystal when the edge dislocation moves from the right-hand side of the crystal to the left-hand side of the crystal as a result of the applied shear stress.

When a shear stress is applied to the crystal and causes the dislocation to move, there must be an equivalent force acting on the dislocation to cause the dislocation motion. We label as F_d this equivalent force on the dislocation due to the applied stress. The unit of F_d is force per unit length of dislocation (N/m; this unit is not to be confused with that of stress, N/m²). We can understand the meaning of a force on dislocation by noting that F_d is a direct result of an applied shear stress which causes the dislocation to move. Since the dislocation moves due to F_d across the slip plane, the work done by the dislocation, W_d , is

$$W_d = F_d l D. \quad (6.22)$$

To check the consistency of units, we note that work done is in units of N-m and l and D are in units of meters, conforming that F_d has the units of N/m.

The force F_d on the dislocation causes the dislocation to travel from the right-hand side to the left-hand side of the crystal. Since this movement of the dislocation across the crystal causes the crystal to slip by an amount b , the work done by dislocation is equal to the work done by the shear stress on the crystal:

$$W_d = W_\tau. \quad (6.23)$$

Therefore,

$$F_d = \tau b. \quad (6.24)$$

The force on the dislocation results from the applied shear stress on the crystal, and the resulting force acts normal to the dislocation. For a screw dislocation, F_d is also given by $F_d = \tau b$ and acts normal to the dislocation.

6.5.2 Stress Field Around Dislocations

Dislocations are essentially due to atoms out of normal registry. At the core of a dislocation, the atomic arrangement may be quite disruptive. At some distance from the core of the dislocation, the atoms tend to return to registry. As a result of the gradual decay of the disruptive atomic arrangement away from the core, the lattice around a dislocation is strained more severely near the core and less so away from the core. The elastic stress associated with the strain therefore follows the same trend. As in Chapter 1, the strain is dl/l .

Consider a screw dislocation lying along an arbitrary direction, z (Fig. 6.22). We assume that the lattice is isotropic where the elastic constants are independent

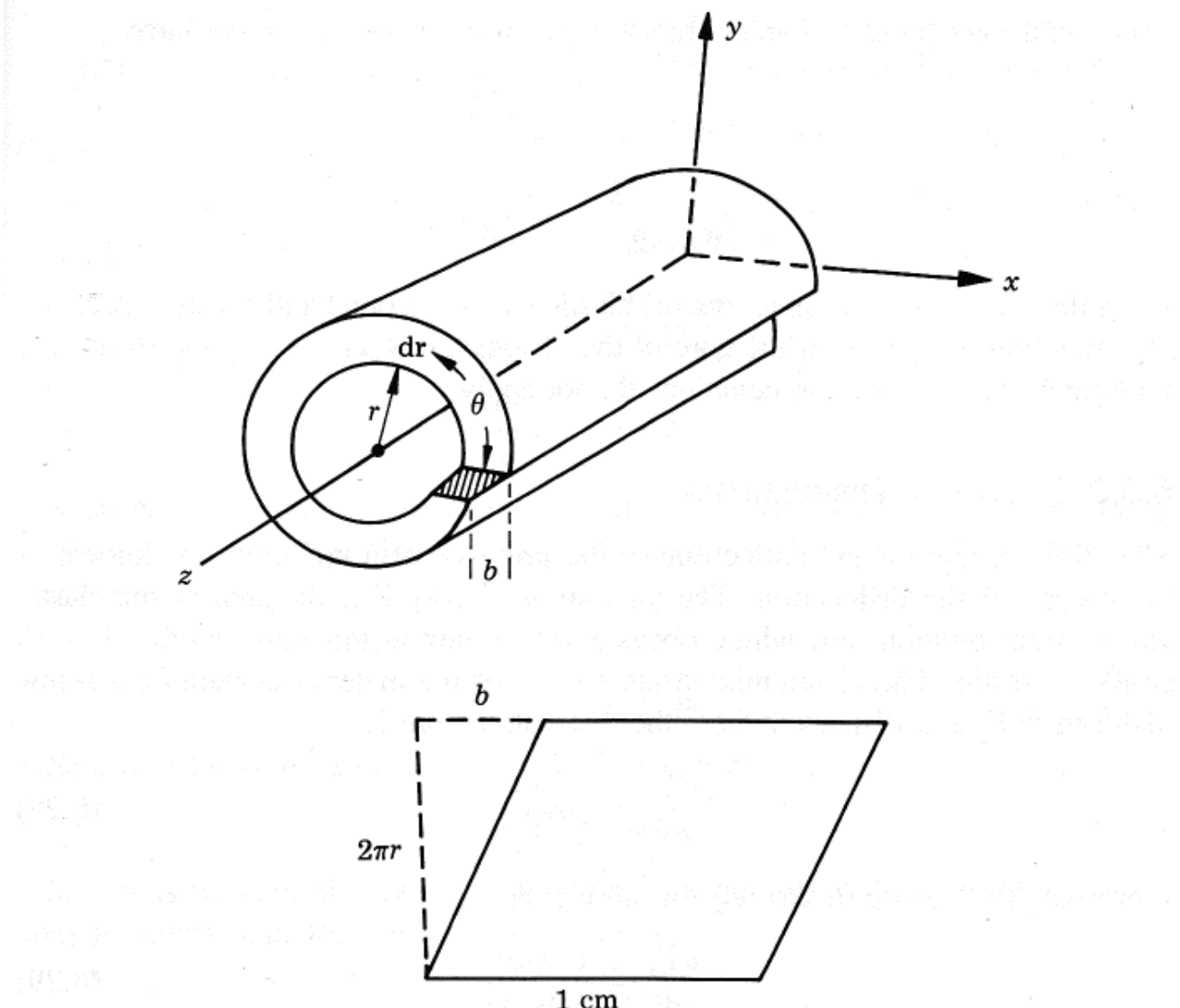


FIGURE 6.22 Displacement around a screw dislocation lying on an arbitrary z axis. The lower drawing shows the “unfolded” material around the dislocation.

of the orientation of the crystal axis. If we “unfold” a shell of material with thickness dr at a distance r away from the screw dislocation, it is clear that a shear strain is associated with the material surrounding the dislocation due to the Burgers vector. The shear strain is given by

$$\varepsilon_{\theta z} = \frac{b}{2\pi r} \quad r > b \quad (6.25)$$

where we use the subscript θ to indicate cylindrical coordinates and z to indicate the direction of displacement.

The shear stress is given by Hooke’s law,

$$\sigma_{\theta z} = G\varepsilon_{\theta z} = \frac{Gb}{2\pi r} \quad (6.26)$$

where G is the shear modulus of the material. In isotropic materials, $G = \frac{Y}{2(1 + \mu)}$ where Y is Young’s modulus and μ is Poisson’s ratio. Transforming the

stress field into the Cartesian coordinate system (x, y, z system), we have

$$\begin{aligned}\sigma_{zx} &= -\frac{Gb}{2\pi} \frac{y}{x^2 + y^2} \\ \sigma_{zy} &= \frac{Gb}{2\pi} \frac{x}{x^2 + y^2}.\end{aligned}\quad (6.27)$$

From these equations we note that the elastic stresses around a dislocation decrease as a function of $1/r$. Near the core of the dislocation where $r \approx b$, the strains are no longer elastic and these equations do not apply.



6.5.3 Energy of Dislocations

The strain energy of the lattice due to the presence of a dislocation is known as the energy of the dislocation. The total strain energy Γ is the area of the elastic stress-strain relationship, which obeys Hooke's law in this case, so that $\Gamma = \frac{1}{2}$ stress \times strain. The differential strain energy of the material containing a screw dislocation Γ_s at a distance r from the dislocation core is

$$\frac{d\Gamma_s}{dV} = \frac{1}{2} \sigma_{\theta z} \varepsilon_{\theta z}. \quad (6.28)$$

From eqs. (6.25) and (6.26), eq. (6.28) can be written

$$\frac{d\Gamma_s}{dV} = \frac{1}{2} \frac{Gb^2}{4\pi^2 r^2} \quad (6.29)$$

where Γ_s is the total energy of the screw dislocation per unit length of the screw dislocation and V is the volume of the material.

$$\begin{aligned}d\Gamma_s &= \frac{1}{2} \frac{Gb^2}{4\pi^2 r^2} dV = \frac{1}{2} \frac{Gb^2}{4\pi^2 r^2} 2\pi r dr \\ &= \frac{Gb^2}{4\pi} \frac{dr}{r}\end{aligned}\quad (6.30)$$

$$\Gamma_s = \int_{r_c}^r \frac{Gb^2}{4\pi} \frac{dr}{r} + U_c \quad (6.31)$$

where r_c is the radius of the dislocation core ($r_c \approx b$) and U_c is the energy of the dislocation core where elasticity theory does not hold. Upon integration, we have

$$\Gamma_s = \frac{Gb^2}{4\pi} \ln \frac{r}{b} + U_c. \quad (6.32)$$

U_c is estimated to be between $Gb^2/12$ and $Gb^2/5$ (liquid-like atomic arrangement; thus U_c is estimated by the heat of fusion). Assuming that $U_c \approx 2(Gb^2/4\pi)$, twice the lower limit, we obtain

$$\Gamma_s = \frac{Gb^2}{4\pi} \left(\ln \frac{r}{b} + 2 \right). \quad (6.33)$$

We note that the strain energy increases as $\ln r$. For a well-annealed metallic crystal where the dislocation density ρ is about $10^8/\text{cm}^2$, the average distance L between two dislocations is 10^{-4} cm ($L \simeq \frac{1}{\sqrt{\rho}}$). If these two dislocations are of the opposite signs, their stress fields approximately cancel each other at middistance (i.e., $r = L$). Using $b = 10^{-8}$ cm, this approximation leads to

$$\begin{aligned}\Gamma_s &= \frac{Gb^2}{4\pi} \left(\ln \frac{10^{-4} \text{ cm}}{10^{-8} \text{ cm}} + 2 \right) \\ &\simeq \frac{Gb^2}{4\pi} (12) \simeq Gb^2.\end{aligned}\quad (6.34)$$

For an edge dislocation, the dislocation energy is modified by Poisson's ratio μ (Poisson's ratio = lateral strain/longitudinal strain). The energy for an edge dislocation Γ_e is

$$\Gamma_e = \frac{\Gamma_s}{1 - \mu} \quad (6.35)$$

where μ is Poisson's ratio. In general, the strain energy

$$\Gamma = \alpha Gb^2 \quad (6.36)$$

where α is between 0.5 and 1. For semiconductors where the dislocation density may be lower than $100/\text{cm}^2$, and $L \simeq 0.1$ cm,

$$\begin{aligned}\Gamma &\simeq \frac{Gb^2}{4\pi} \left(\ln \frac{0.1 \text{ cm}}{10^{-8} \text{ cm}} + 2 \right) \\ &\simeq 1.5Gb^2.\end{aligned}\quad (6.37)$$

It should be noted that Γ is not a very sensitive function of the dislocation density due to the logarithmic dependence of r (or the size of the crystal). For Si, $G = 7.5 \times 10^{10}$ N/m², $b = (a/2) [110]$, and $a = 0.543$ nm, the dislocation energy (in units of eV/length of dislocation) is about 10.4 eV per 0.1 nm. This is a very large amount of energy, and therefore it is very difficult to create dislocations by random thermal fluctuations. Dislocations are created by stresses during thermal and mechanical processing and during crystal growth.

6.5.4 Electronic Effects of Dislocations

The single dangling electron at each atomic site along an edge dislocation in Si and Ge is usually considered as an acceptor, attracting an electron to lower its energy from E_1 to E_2 (Fig. 6.23). Thus the core of the edge dislocation may be negatively charged and repels electrons, thus forming a positively charged space which obstructs the transport of free electrons in the material (Mataré, 1971).

Consider an *n*-type semiconductor with a net donor concentration of $(N_D - N_A)$. For a negatively charged dislocation line, a positively charged cylinder of radius R will be formed around the dislocation such that

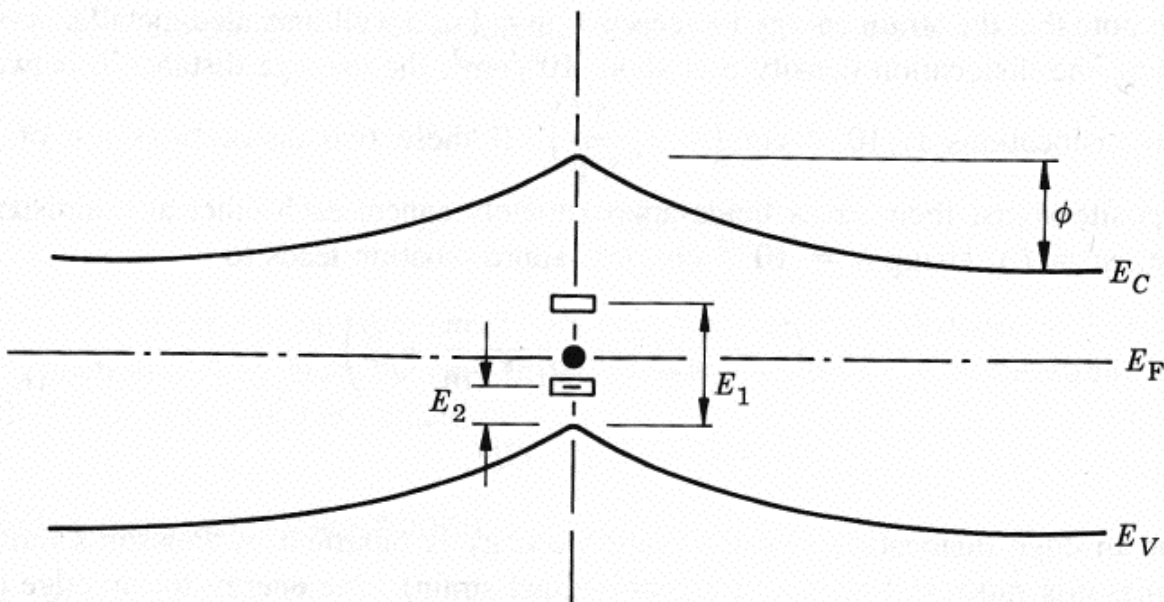


FIGURE 6.23 Band bending around an edge dislocation. The dangling electron at the core of the dislocation (running into the page) accepts an electron to lower its energy from E_1 (relative to E_V) to E_2 , forming a positively charged space-charge region. The electron barrier ϕ is created (band bending) around the dislocation to repel the free electrons in the semiconductor. [After Mataré (1971).]

$$e\pi R^2(N_D - N_A) = \frac{e}{d} = \frac{ef}{c} \quad (6.38)$$

where e is the electronic charge, f the filling factor (or the probability of an electron occupying the state), c the spacing between the dangling bonds, and d the distance between filled states.

$$f = \frac{c}{d} = \frac{1}{1 + \exp [(E_2 - E_F)/kT]}. \quad (6.39a)$$

The left-hand side of eq. (6.38) is due to the positive charge in the cylinder, and the right-hand side is due to the negative line charge at the dislocation core. The spacing between the dangling bonds, c , is

$$c \approx \frac{a}{\sin \alpha} \quad (6.39b)$$

where α is the angle between the Burgers vector \mathbf{b} and the dislocation line and a is the lattice spacing. For a screw dislocation $\alpha = 0$, $c \rightarrow \infty$, there are no dangling bonds and a space-charge region does not form. For an edge dislocation, $\alpha = 90^\circ$, $c \approx a$. Rearranging eq. (6.38) yields

$$\begin{aligned} R &= [d\pi(N_D - N_A)]^{-1/2} \\ &= \left[\frac{f}{c} \frac{1}{\pi(N_D - N_A)} \right]^{1/2} \\ &= \left\{ \frac{[1 + \exp ((E_2 - E_F)/kT)]^{-1}}{c\pi(N_D - N_A)} \right\}^{1/2}. \end{aligned} \quad (6.40)$$

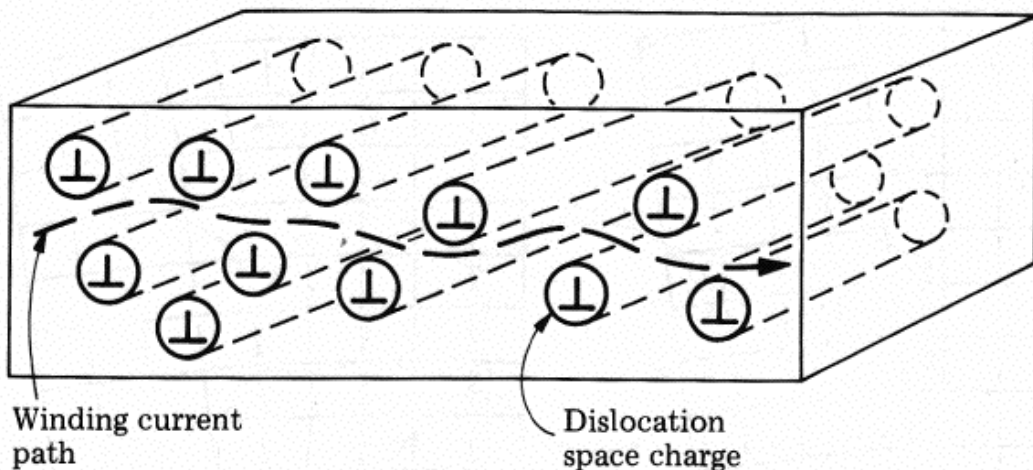


FIGURE 6.24 Current transport in a semiconductor containing dislocation space-charge cylinders. [After Mataré (1971).]

Assuming that $f \approx 0.5$ and $c \approx 10^{-7}$ cm, we have $R \approx 4$ to $5\text{ }\mu\text{m}$. With a space-charge region around each dislocation, the transport of carriers normal to the dislocation lines would be affected due to the winding current path, resulting in increased resistivity and reduced carrier mobility. The transport of carriers parallel to the dislocation lines is affected to a lesser amount (see Fig. 6.24).

In addition to the space-charge effects, dislocations may act as generation–recombination centers for carriers. Referring to Fig. 6.23, the dangling bond at the dislocation is negatively charged after accepting an electron to lower its energy. The trapped state (E_2) is therefore attractive to the holes. If a hole is captured, the previously captured electron will be annihilated by the captured hole. The dangling bond state goes back up to E_1 and the entire process can be repeated (recombination via the dislocation core state). The issue of the recombination–generation processes has been discussed in Chapter 3. The presence of dislocations across a p - n junction causes excessive leakage current, partially due to the recombination process at dislocation core states and partially due to the gettering of metallic impurities along the core, thus forming a conductive path. The electronic behavior of dislocations in GaAs is not firmly established. It is believed that they may be electronically active as recombination centers, similar to those in Si and Ge.

6.6 Planar Defects

Planar defects include grain boundaries, stacking faults, and twins. These defects are formed during crystal growth and/or during thermal and mechanical processing of the semiconductor. All three types of planar defects are enclosed by a single dislocation or an array of dislocations separating the faulted area from the normal area or delineating the misorientation between various areas of the semiconductor. In general, these defects are not beneficial to device operations; however, under certain circumstances they may be used to “getter” deep level impurities in the semiconductor.

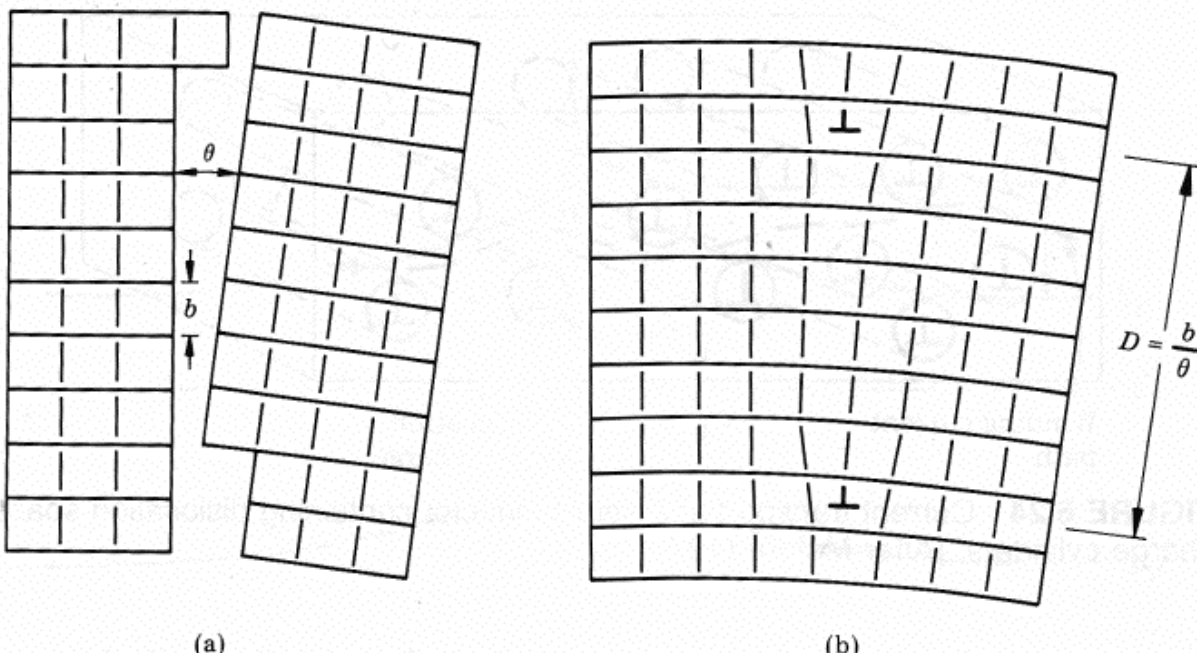


FIGURE 6.25 (a) Simple grain boundary. The plane of the figure is parallel to a cube face and normal to the axis of relative rotation of the two grains. (a) Two grains have a common cube axis and an angular difference in orientation θ . (b) The two grains are joined to form a bicrystal. The joining requires only elastic strain except where a plane of atoms ends on the boundary in an edge dislocation, denoted by the symbol \perp . [After Read (1953).]

6.6.1 Grain Boundaries

Grain boundaries are not expected to exist in single-crystalline materials; however, in certain devices, such as the polysilicon solar cells, a polycrystalline semiconductor is used. A grain boundary may be viewed as an array of dislocations separating two single grains of crystalline material with a misorientation between them (Fig. 6.25). A tilt boundary is formed when the dislocation array is composed of edge dislocations only; a twist boundary is formed when the array is composed of screw dislocations only (Read, 1953). The misorientation between the adjacent grains increases as the number of dislocations composing the grain boundary increases. Since each dislocation has an energy associated with it [eq. (6.36)], the grain boundary energy should increase with increasing misorientation until the stress fields of the dislocations start to cancel due to overlaps. For a general grain boundary, the structure of the boundary may be modeled as part tilt and part twist.

Electronic states in the semiconductor band gap have been associated with dislocations, resulting in a space region around the dislocation core. It is not surprising that space-charge regions are associated with grain boundaries. The electrical conductivity in a polycrystalline sample is expected in general to be larger in the direction parallel to the grain boundary than that normal to it (Mataré, 1984), similar to what is observed for dislocations (Fig. 6.24).

6.6.2 Stacking Faults and Twins

The $\{111\}$ planes of FCC crystals have a normal stacking sequence of $\cdots \text{ABC ABC} \cdots$ (Fig. 6.26). If an extra $\{111\}$ -A plane is inserted between a $\{111\}$ -B and

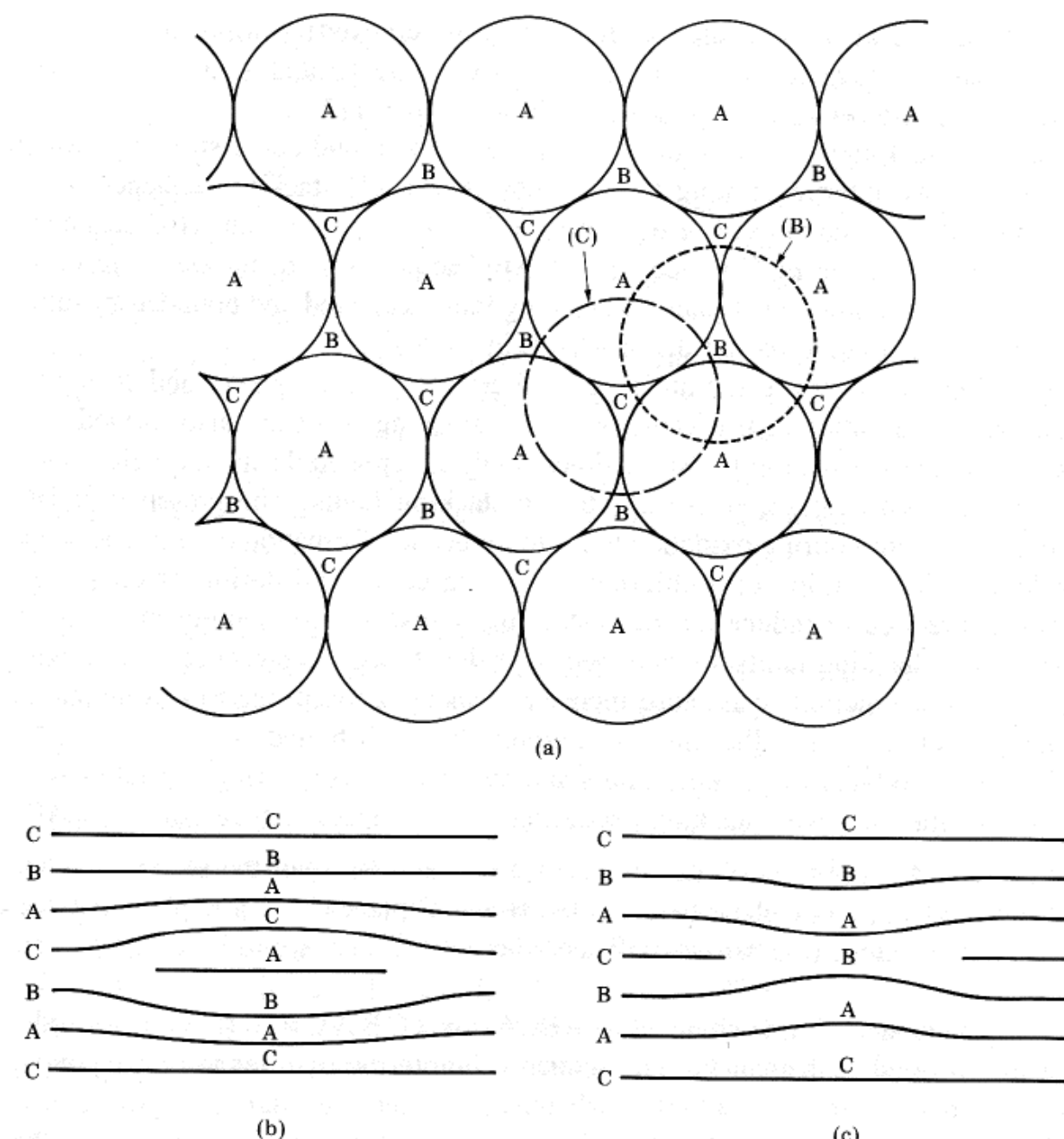


FIGURE 6.26 Stacking spheres in close packing. (a) When one close-packed layer has been laid down (the A layer), the next layer can go into either of the two sets of hollows (B or C) on the first layer. A, B, and C denote the centers of the spheres in the three possible positions. The normal FCC stacking sequence of the {111} plane is . . . ABCABC. . . . The normal hexagonal close-packed stacking sequence of the basal plane is . . . ABAB. . . . (b) Extrinsic stacking fault: a {111}-A plane is inserted between a {111}-B plane and a {111}-C plane. (c) Intrinsic stacking fault: a {111}-C plane is removed between a {111}-B plane and a {111}-A plane.

a {111}-C plane, the stacking sequence is now changed to AB AC (the arrow indicates the inserted plane), the stacking of the first three {111} planes has the sequence ABA, which is not the normal stacking of the FCC crystals but of the hexagonal close-packed (HCP) crystals. An *extrinsic* stacking fault is said to have formed. The faulted area is bounded by a Frank partial dislocation with a Burgers vector of $\mathbf{b} = (a/3) \langle 111 \rangle$, a Burgers vector of magnitude $a/3$ lying along the $\langle 111 \rangle$ direction. If a {111}-C plane is removed between a {111}-B plane and a {111}-A plane from the ABC sequence, the stacking sequence is changed to

$\text{AB} \uparrow \text{ABC}$ (the arrow indicates where a plane is removed). An *intrinsic* stacking fault is said to have formed and the boundary of the faulted area is a Shockley partial dislocation with a Burgers vector $\mathbf{b} = (a/6) <112>$.

Semiconductors such as Si and GaAs have the diamond cubic structure, which consists of two interpenetrating FCC lattices. The {111} stacking sequence of the diamond lattice is composed of three double {111} planes with an ABC sequence, similar to that of the FCC lattice. If this ABC sequence is disturbed by inserting or removing a double-{111} plane, a stacking fault is created and bounded by either a Frank or a Shockley partial dislocation (Fig. 6.26).

Stacking faults are created during crystal growth such as epitaxy and during the annealing of ion implanted regions. Extrinsic stacking faults are also formed in Si due to oxidation. Apparently, Si self-interstitials are created during oxidation; these interstitials then coalesce to form extrinsic stacking faults. The presence of HCl (actually chlorine) during oxidation tends to reduce the formation of extrinsic stacking faults. The addition of a chlorine-containing compound during oxidation is a common practice to reduce not only stacking faults but also sodium in the oxide layer. Since stacking faults are bounded by dislocations, the presence of a stacking fault near *p-n* junctions can cause increased leakage current due to recombination and/or gettering of metallic impurities around the fault boundaries.

Twins are related to stacking faults and are also formed during crystal growth. Consider the normal stacking sequence of a FCC lattice of $\cdots \text{ABC}$
 $\text{A} \downarrow \text{B} \downarrow \text{C} \downarrow \text{A} \downarrow \text{B} \downarrow \text{C} \cdots$. Let us insert a C plane between the second A plane and the B plane, an A plane between the B and C planes, and a B plane between the C and B planes (the arrows indicate where the planes are to be inserted). The

$\downarrow \quad \downarrow \quad \downarrow \quad \downarrow \quad \downarrow$

stacking sequence is now changed to ABCACBACBACBA (the arrows indicate the inserted fault planes). The sequence before the twin plane (the second A plane from the left) is ABCABC, whereas the sequence after the twin plane is ACBACB. A twin fault is therefore formed by inserting a fault plane every other plane in the normal FCC stacking sequence ("a twin is a many-faulted thing"). Despite the fact that a twin can be created by inserting many fault planes, the FCC lattice stacking sequence is undisturbed before and after the twin plane. The influence of twins on the electronic device performance has been reported to be less significant than that of the stacking faults.

6.7 Volume Defects

Volume defects include voids and local regions of different phases, such as a precipitate or an amorphous phase. In Si, oxygen precipitation is the most important volume defect. Silicon crystals are grown by either the Czochralski technique (Chapter 1) or by the float-zone technique. The typical concentration of oxygen in Czochralski Si crystal is about 10 to 20 ppm (parts per million) or 5×10^{17} to $1 \times 10^{18} \text{ cm}^{-3}$. The float-zone technique introduces less oxygen in Si than does the Czochralski technique. Most of the oxygen in the as-grown crystal is atomically dispersed and occupies interstitial sites. A low-temperature annealing at 300 to

500°C causes the interstitial oxygen to move into substitutional sites and become donors. An increase in donor concentration during the packaging and passivation steps of an MOS (metal–oxide Si) device at $\approx 450^\circ\text{C}$ causes a drastic change of the threshold voltage of the devices (Wolf and Tauber, 1986). These oxygen donors must be reduced or eliminated by a precipitation step of annealing at 600 to 700°C or at an elevated temperature cycle of about 1100°C. The high-temperature cycle of forming SiO_2 precipitates in Si is the basic method used for intrinsic gettering, an issue discussed in the following section.

For precipitation to occur, we need (1) a thermodynamic driving force for the precipitation reaction—this driving force (a deviation from equilibrium) is generally in the form of a supersaturation of the solute atoms or in terms of a chemical reaction such as the formation of SiO_2 , and (2) atomic mobility—solute atoms must be able to diffuse to the nucleation sites such as dislocations (heterogeneous nucleation) or diffuse together to form nuclei by themselves (homogeneous nucleation).

Other than oxygen precipitates, metallic precipitates of Cu, Co, Ni, and Fe are observed to form and to serve as nucleation sites for stacking faults during epitaxial growth. These impurity precipitates need to be “gettered” for suitable device operation.

Another type of volume defect is due to local amorphous regions encountered in ion-implanted semiconductors, especially in the case of low-dose irradiation where local amorphous regions around the ion tracks do not overlap to form a continuous layer. The amorphous phase can be considered as a structure without long-range order. Figure 6.27 shows the schematic atomic arrangement for an amorphous solid and for a crystalline solid. As one can see, a crystalline solid has long-range atomic order; an amorphous solid has short-range order (the order among the nearest neighbors) but no long-range order (Elliott, 1986). This type of volume defect is readily eliminated by an annealing step, as discussed in Chapter 8.

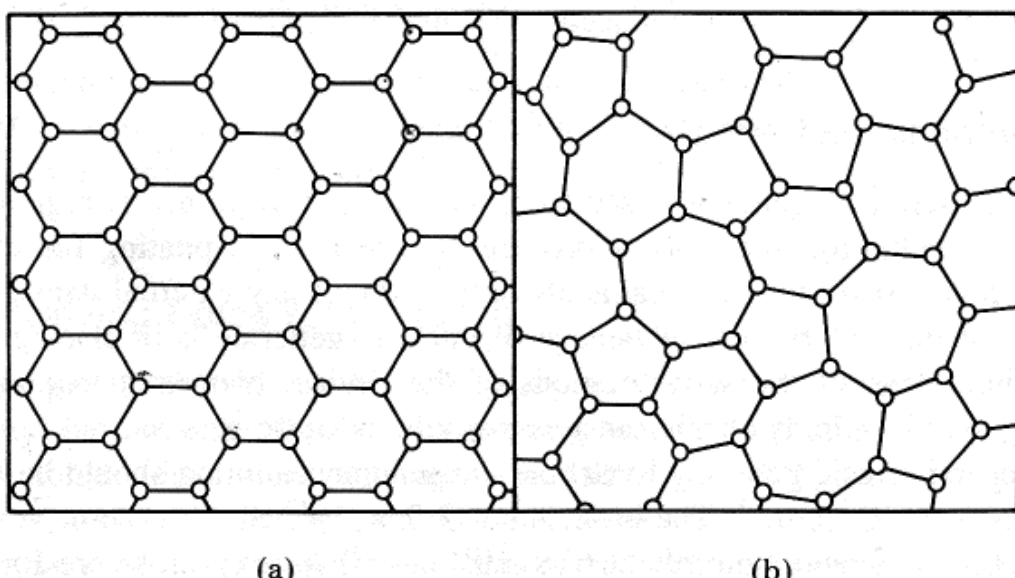


FIGURE 6.27 Schematic atomic arrangement of (a) a crystalline solid and (b) an amorphous solid.

6.8 Gettering in Si

As discussed previously, defects and impurities in semiconductors adversely affect the performance of the devices. To improve electronic performance, a processing step known as “gettering” is practiced, especially in Si technology. The basic principle of gettering is utilization of the stress fields of strategically located dislocations to capture impurities at moderate processing temperatures. The dislocations may be introduced by external means on the back side of wafers, known as extrinsic gettering, or from an internal source by creating dislocations away from the active regions of the device, known as intrinsic gettering. For gettering to occur, it is necessary for impurity atoms in the form of a precipitate to (1) dissolve into the host semiconductor, (2) diffuse toward dislocations due to the attractive forces between them, (3) form a precipitate around the dislocation in an inactive region of the semiconductor, and (4) remain without release into the host semiconductor during subsequent processing steps.

6.8.1 Extrinsic Gettering

In extrinsic gettering, dislocations are introduced by external means at the back side of wafers. The common methods to introduce dislocations include laser-induced damage, mechanical abrasion, ion implantation, high concentration diffusion, and the deposition of a layer of polysilicon (Wolf and Tauber, 1986). The introduction of dislocations by laser and mechanical abrasion is clearly due to damage. Ion implantation with the proper ions introduces not only dislocations but also planar defects such as stacking faults (Cullis et al., 1978). The diffusion of P from the backside with high surface concentration causes a change in the Si lattice parameter; dislocations are created to accommodate the change (Tseng et al., 1978). These dislocations then act as gettering sites. In the case of deposited polysilicon, the grain boundaries are essentially the active sites for gettering. It should be noted that polysilicon undergoes grain growth at the temperature of gettering, thus causing the gettering efficiency to be reduced.

6.8.2 Intrinsic Gettering

Intrinsic gettering is generally used to remove oxygen from active regions of Si. In intrinsic gettering, the dislocations are created by precipitating the dissolved oxygen in the Si using heat treatments only, without any external damage to the backside of the wafers. The advantage of intrinsic gettering is in placing the gettering sites close to the active regions of the device, compared to placing the gettering sites hundreds of micrometers away in extrinsic gettering.

To apply intrinsic gettering to Si, the oxygen concentration should be between 7.5 and $9.5 \times 10^{17} \text{ cm}^{-3}$. The lower limit ($7.5 \times 10^{17} \text{ cm}^{-3}$) is somewhat above the threshold concentration (about $6 \times 10^{17} \text{ cm}^{-3}$) for oxygen to precipitate and the upper limit ($9.5 \times 10^{17} \text{ cm}^{-3}$) is below the concentration where oxygen precipitation results in such a high density of precipitates that the wafers may warp

and may generate gettering sites in the active-device regions (Wolf and Tauber, 1986). The control of the oxygen concentration in the wafers should be rather precise for intrinsic gettering to apply.

Under appropriate heat treatment, the oxygen in the Si precipitates out to form SiO_2 . There is a large volume change associated with the formation of SiO_2 (the volume of SiO_2 /volume of Si ratio is about 2). To accommodate the compressive stress generated by the presence of SiO_2 particles, several stress-releasing mechanisms are involved: (1) formation of dislocation loops, (2) emission of Si self-interstitials, and (3) absorption of vacancies. The Si self-interstitials have the tendency to form extrinsic stacking faults with dislocations as fault boundaries. As a result of the dislocations generated by formation of SiO_2 particles, gettering sites become available. The issue now is how to place the SiO_2 particles away from the active-device region for gettering purposes. It has been observed that a three-step annealing cycle can achieve intrinsic gettering in a wafer having uniformly distributed oxygen of the appropriate concentration. A three-step high-low-high annealing sequence is described by Wolf and Tauber (1986):

1. A high-temperature annealing (about 1100°C, for example) to reduce the oxygen concentration near the wafer surface. This step is taken to cause out-diffusion of the oxygen from the surface region, thus reducing the oxygen concentration to about the solubility limit at the processing temperature. The depth of the “denuded” zone should exceed that of the deepest *p-n* junction.
2. A low-temperature annealing (600 to 800°C, for example) to nucleate SiO_x precipitates. This annealing step for prolonged periods (e.g., 4 to 64 hours) causes the supersaturated interstitial oxygen to diffuse in a local region and nucleate into small clusters.
3. A high-temperature annealing (900 to 1250°C) for extended periods (4 to 16 hours) to cause growth of SiO_2 nuclei. The growth of small clusters to large nuclei (50 to 100 nm) causes the generation of dislocations by forming prismatic dislocation loops and by emitting Si self-interstitials, which coalesce to form extrinsic stacking faults. The gettering sites are thereby created by this three-step annealing sequence.

Although intrinsic gettering is an elegant technique, it does require strict control of process parameters. It is a common practice to implement both extrinsic and intrinsic gettering concurrently.

6.8.3 Driving Force for Gettering

Let us consider the driving force of gettering due to the interactions between an impurity and an edge dislocation. Suppose that in a semiconductor there are n substitutional solute atoms with atomic radius R_1 ($R_1 \neq R_{\text{host}}$). The solute atoms therefore introduce dilatation or contraction into the lattice. Such strain centers interact with the hydrostatic stress fields of dislocations in the crystal. The hydrostatic stress field (either in tension or in compression) is due to the normal stresses associated with a dislocation.

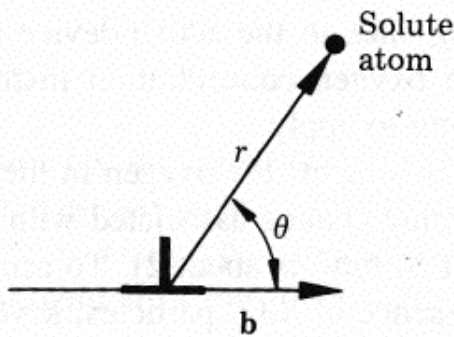


FIGURE 6.28 Interaction between a solute atom and an edge dislocation. The dislocation runs perpendicular to the plane of paper (z direction). The solute atom is located at r and θ with respect to the dislocation. The angle θ is the angle between the direction of the Burgers vector \mathbf{b} and the direction r .

The normal stress field of an edge dislocation in cylindrical coordinate system is given by

$$\sigma_{rr} = \sigma_{\theta\theta} = -\frac{Gb \sin \theta}{2\pi(1 - \mu)r} \quad (6.41)$$

where G is the shear modulus and μ is Poisson's ratio (see Section 6.5.2). These stresses are either in compression or tension, depending on the angle θ which is defined by the angle between the direction of the Burgers vector and the direction r (Fig. 6.28). There is a normal stress in the z direction (along the dislocation line) associated with an edge dislocation. This normal stress is

$$\sigma_{zz} = \mu(\sigma_{\theta\theta} + \sigma_{rr}). \quad (6.42)$$

There is also a shear stress field around an edge dislocation just as those around a screw dislocation [eq. (6.26)]. The mean hydrostatic stress field of an edge dislocation may be taken as the average of the three normal stresses associated with an edge dislocation. The mean hydrostatic stress, P_{edge} , is

$$\begin{aligned} P_{\text{edge}} &= \frac{\sigma_{rr} + \sigma_{\theta\theta} + \sigma_{zz}}{3} \\ &= \frac{1 + \mu}{3} (\sigma_{rr} + \sigma_{\theta\theta}) \\ &= \frac{-(1 + \mu)Gb \sin \theta}{3\pi(1 - \mu)r} \end{aligned} \quad (6.43)$$

where μ is Poisson's ratio, G is the shear modulus, and r and θ are the positions of the solute atom with respect to the dislocation line (Fig. 6.28). Screw dislocations produce only shear stress field, no hydrostatic stress. Substitutional solute atoms do not interact with screw dislocations. Interstitial atoms produce both shear and hydrostatic stress in the lattice; therefore, they interact with both screw and edge dislocations.

The work done, W , to increase the size from that of a host atom R to R_1 (radius of a solute atom) against the constant mean hydrostatic stress of an edge dislocation is

$$\begin{aligned} W &= P_{\text{edge}} \Delta V = P_{\text{edge}} \Delta \left(\frac{4}{3} \pi R^3 \right) = P_{\text{edge}} 4\pi R^2 \Delta R \\ &= \frac{-(1 + \mu)Gb \sin \theta}{3\pi(1 - \mu)r} 4\pi R^2 \frac{R_1 - R}{R}. \end{aligned} \quad (6.44)$$

The interaction energy between a solute atom and an edge dislocation, U , is just equal to the work done, so that

$$U = \frac{-A \sin \theta}{r} \quad (6.45)$$

where

$$A = \frac{-(1 + \mu)Gb}{3\pi(1 - \mu)} \cdot 4\pi R^2 \frac{R_1 - R}{R}.$$

Introducing Cartesian coordinates $r^2 = x^2 + y^2$ and $\sin \theta = y/r$, eq. (6.45) may be written as

$$U = \frac{Ay}{x^2 + y^2} \quad (6.46)$$

$$x^2 + y^2 - \frac{Ay}{U} = 0$$

$$x^2 + \left[y^2 - \frac{Ay}{U} + \left(\frac{A}{2U} \right)^2 \right] - \left(\frac{A}{2U} \right)^2 = 0$$

which can be expressed as

$$x^2 + (y')^2 = \left(\frac{A}{2U} \right)^2 \quad (6.47)$$

where

$$y' = y - \frac{A}{2U}$$

Each constant interaction energy is represented by a circle, tangent to the line $y = 0$ and centered on the line $x = 0$, as shown in Fig. 6.29. The interaction force to which the solute atoms is subjected acts normal to the equi-energy lines in the direction of the conjugate set of circles, shown as dashed curves. Solute atoms larger than the host will migrate to the lower part of the dislocation in the direction shown by the arrow. Solute atoms smaller than the host will migrate in the opposite direction. The driving force for gettering by dislocation is essentially due to the interaction energy, shown in eq. (6.47).

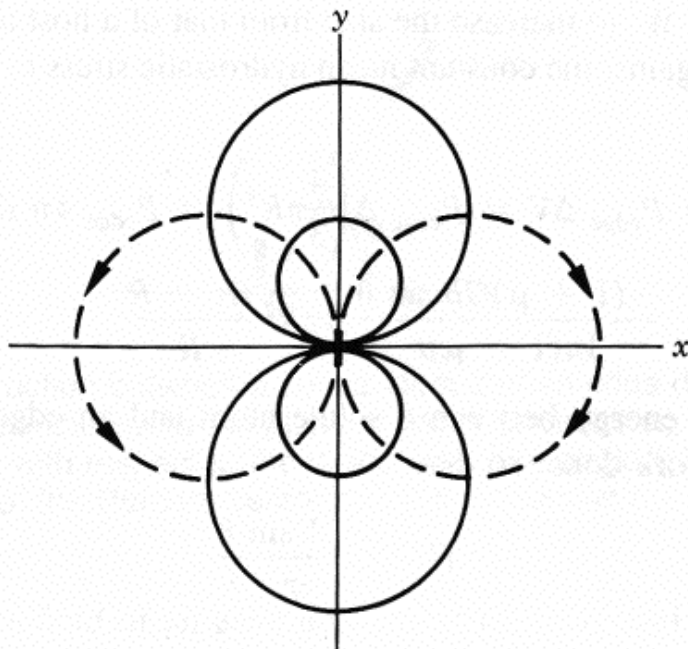


FIGURE 6.29 Circles of constant interaction energy.

REFERENCES

General References

- CASEY, H. C., JR., and M. B. PANISH, *Heterostructure Lasers*, Academic Press, New York, 1978.
- CULLITY, B. D., *Elements of X-Ray Diffraction*, Addison-Wesley, Reading, Mass., 1956, Chapter 2.
- ELLIOTT, S. R., *Physics of Amorphous Materials*, Wiley, New York, 1986.
- HIRTH, J. P., and J. LOTHE, *Theory of Dislocations*, McGraw-Hill, New York, 1968, Chapter 2.
- KIRKPATRICK, C. G., R. T. CHEN, D. E. HOLMES, and K. R. ELLIOT, "Growth of Bulk GaAs," in *Gallium Arsenide, Materials, Devices, and Circuits*, ed. M. J. Howes and D. V. Morgan, Wiley, New York, 1985.
- MATARE, H. F., *Defect Electronics in Semiconductors*, Wiley-Interscience, New York, 1971, Chapters 8 and 10.
- READ, W. T., *Dislocations in Crystals*, McGraw-Hill, New York, 1953.
- WOLF, S., and R. N. TAUBER, *Silicon Processing for VLSI Era*, Vol. 1, *Processing Technology*, Lattice Press, Sunset Beach, California, 1986, Chapter 2.

Specific References

- CULLIS, A. G., T. E. SEIDEL, and R. L. MEEK, *J. Appl. Phys.* 49, 5188 (1978).
- FAHEY, P. M., "Point Defects and Dopant Diffusion in Silicon," Ph.D. thesis, Stanford University, 1985.
- GHANDI, S. K., "VLSI Fabrication Principles, Silicon and Gallium Arsenide," *VLSI Fabrication Principles. Silicon and Gallium Arsenide*, Wiley, New York, 1983.
- JENKINS, M. W., *J. Electrochem Soc.* 124, 757 (1977).

- LAGOWSKI, J., H. C. GATOS, J. M. PARSEY, K. WODA, M. KAMINSKI, and W. WALAKEIWICZ, *Appl. Phys. Lett.* 40, 342 (1982).
- LANG, D. V., *J. Appl. Phys.* 45(7), 3023 (1974).
- MATAŘE, H. F., *J. Appl. Phys.* 56(10), 2605 (1984).
- STIRLAND, D. J., *Appl. Phys. Lett.* 53, 2432 (1988).
- TAN, T. Y., and T. K. TICE, *Philos. Mag.* 30, 615 (1976).
- TAN, S. I., B. S. BERRY, and W. F. J. FRANK, in *Ion Implantation in Semiconductors and Other Materials*, ed. B. L. Crowder, Plenum Press, New York, 1973.
- TEENG, W. F., T. KOJI, J. W. MAYER, and T. E. SEIDEL, *Appl. Phys. Lett.* 33(5), 442 (1978).
- VAN VECHTEN, J. A., "A Simple Man's View of the Thermochemistry of Semiconductors," in *Handbook on Semiconductors*, ed. T. S. Moss, Vol. 3, *Materials, Properties and Preparation*, ed., S. P. Keller, North Holland, Amsterdam, 1980, Chapter 1.
- WATKINS, G. D., J. R. TROXELL, and A. P. CHATERJEE, in *Defects and Radiation Effects in Semiconductors 1978*, ed. J. H. Albany, Institute of Physics Conferences Series 46, London, 1979.

PROBLEMS

- 6.1.** Nickel (Ni) is a face-centered cubic (FCC) crystal with an atomic density of 9.14×10^{22} atoms/cm³ and an atomic mass of 58.73.
- (a) What is the mass density (g/cm³)?
 - (b) What is the lattice constant, a ?
 - (c) If $a = 4.0$ Å, what is the distance between (110) planes?
- 6.2.** Silver (Ag) is face-centered cubic with a lattice parameter $a = 4.09$ Å.
- (a) What is the spacing between (123) planes?
 - (b) What is the atomic density of Ag (atoms/cm³)?
 - (c) How many Ag atoms/cm² are in a layer 10^{-4} cm thick?
- 6.3.** Consider a simple cubic crystal and planes with (100), (111), and (110) Miller indices and with an atomic density of 4×10^{22} atoms/cm³.
- (a) Which planes would have the greatest spacing between them?
 - (b) Which planes would have the largest number of atoms/cm² on them?
 - (c) What is the lattice constant a (Å)?
- 6.4.** You have two cubic materials with the same lattice parameter $a = 4.0$ Å. Material A is a simple cubic with atomic mass of 40. Material B is a face-centered cubic with atomic mass of 20.
- (a) Which has the greater atomic density (number of atoms/cm³)?
 - (b) Which has the greater mass density (g/cm³)?
 - (c) Which material has the greater spacing between (100) planes?

- 6.5.** You are given a sphere with a 1-cm radius of the simple cubic material "Cornelian" with an atomic mass of 30. You weigh it and find that it weighs 6.0 g.
- How many atoms are there in the sphere?
 - What is the lattice parameter, a , of the material?
 - You have a 1-cm³ cube of Cornelian and are told that the lattice parameter is 4.0 Å.
 - What is the spacing between (321) planes?
 - How many atoms would be on the outer layer of atoms on the cube?
- 6.6.** Explain why a dislocation must terminate on itself or on a surface or volume fault.
- 6.7.** Show that the diamond cubic lattice has a · · · ABC · · · sequence.
- 6.8.** Explain why summation of the Burgers vector is zero at a dislocation node.
- 6.9.** Based on eqs. (6.17) and (6.18), show that
- $$\frac{[V^\pm]}{[V^x]} = \exp\left(-\frac{E_x^\pm + E_x^- - 2E_F}{kT}\right)$$
- and
- $$\frac{[V^{++}]}{[V^x]} = \exp\left(-\frac{2E_F - E_x^{++} - E_x^-}{kT}\right).$$
- 6.10.** Assuming there are only V^x and V^+ in a semiconductor, show that $[V^+] = [V^x]e^{(E^+ - E_F)/kT}$. (Hint: One may start with $[V_T] = [V^+] + [V^x]$ and recognize that $[V^+]$ is the concentration of positively charged vacancies.)
- 6.11.** The normal stress field around an edge dislocation is given by eq. (6.41). In the Cartesian coordinate system:

$$\sigma_{xx} = -\frac{Gb}{2\pi(1-\mu)} \frac{y(3x^2 + y^2)}{(x^2 + y^2)^2}$$

$$\sigma_{yy} = \frac{Gb}{2\pi(1-\mu)} \frac{y(x^2 - y^2)}{(x^2 + y^2)^2}$$

$$\sigma_{zz} = \mu(\sigma_{xx} + \sigma_{yy})$$

$$\sigma_{xy} = \frac{Gb}{2\pi(1-\mu)} \frac{x(x^2 - y^2)}{(x^2 + y^2)^2}.$$

Work out the sign and direction of the shear stress σ_{xy} and the normal stresses σ_{xx} and σ_{yy} for the cases where $y < x$ and $y > x$.